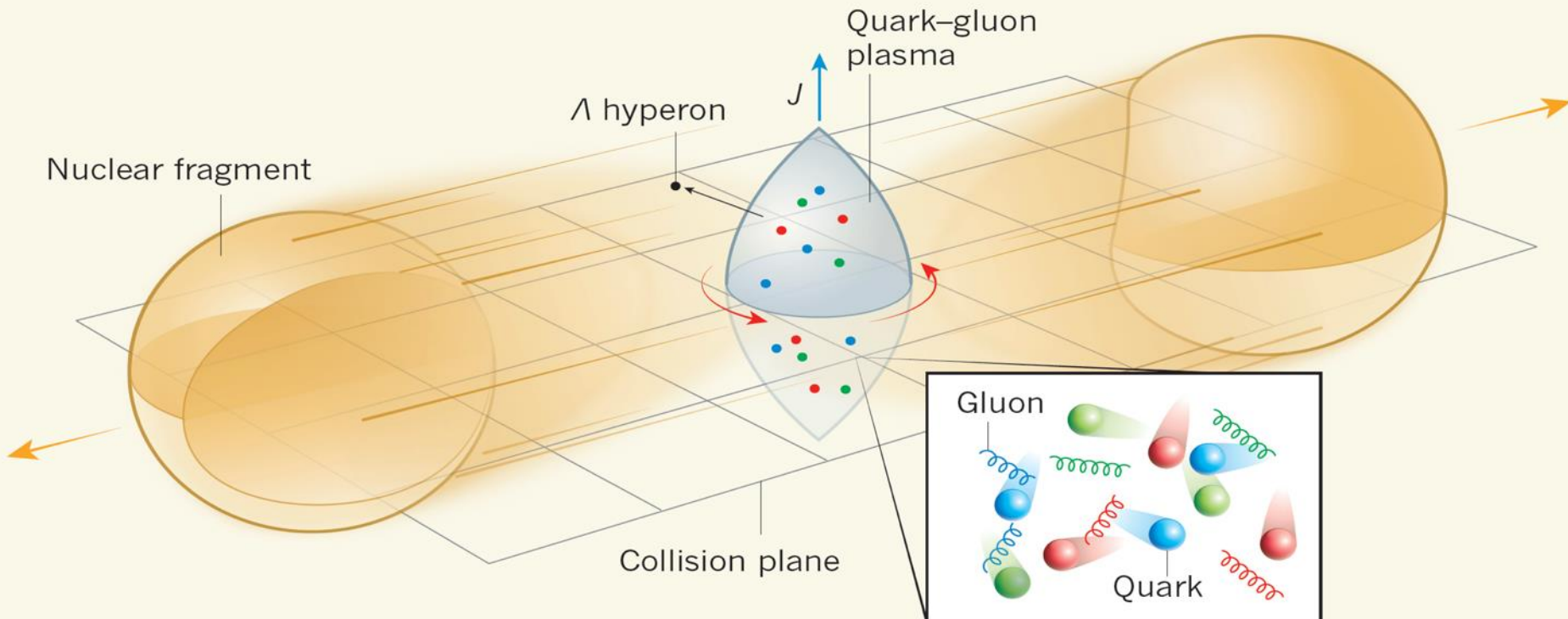


Quark-Gluon Plasma: the Fastest Rotating Fluid



Michal Šumbera

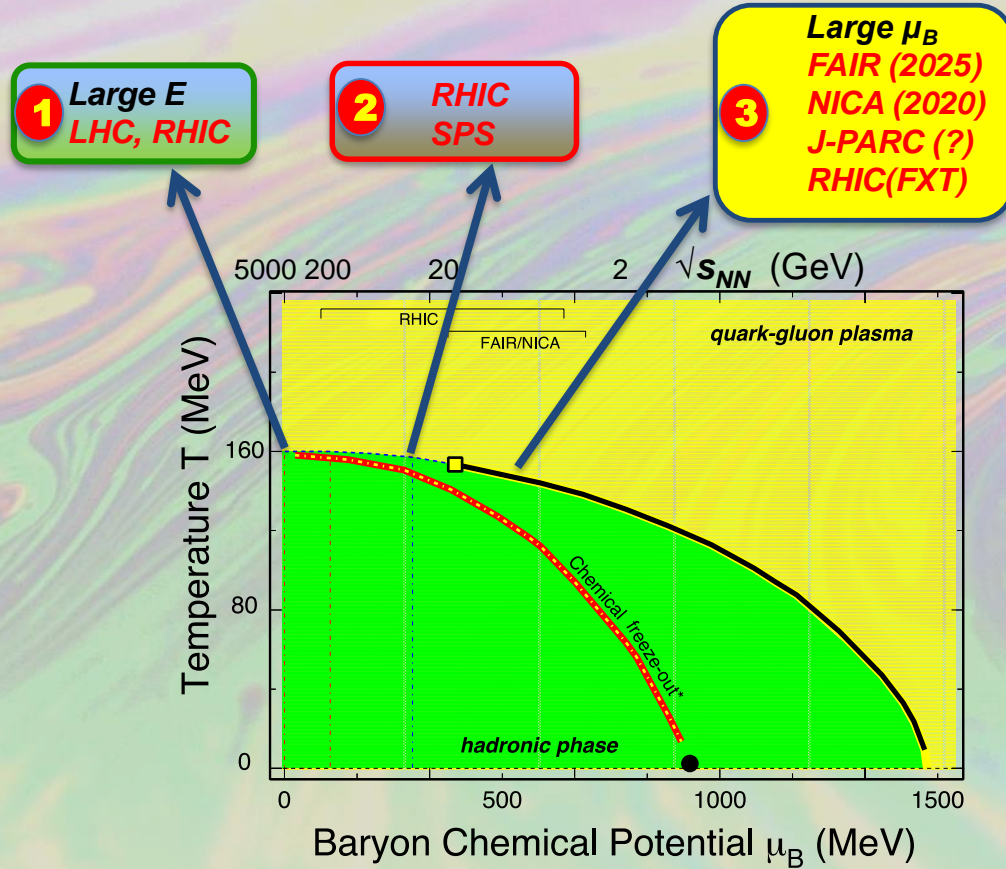
Nuclear Physics Institute of the CAS, Řež/Prague

Figure from Nature 548, 34–35 (03 August 2017)

Outline

- Motivation –subjecting our (hydro) paradigm to scrutiny
- Strong magnetic fields and chiral magnetic effect
- Fluid vorticity and polarization probes
 - Barnett- Einstein-de Haas effects / fluid spintronics
- Hyperon polarization in Beam Energy Scan I
- Extraction of ω & B
 - broader context & comparison with predictions
- Outlook & Summary

The QCD Phase Diagram and BES



2000–2012: RHIC+LHC

Top energy program
Discovery of sQGP

- QCD **Critical Point?**
- Chiral effects?

2010–2017: RHIC BES-I

7.7, 11.5, 14.5, 19.6, 27, 39, 54.4 GeV

2019–2020: RHIC BES-II

7.7, 9.1, 11.5, 14.5, 19.6 GeV

FXT*: 3.0, 3.5, 3.9, 4.5, 7.7 GeV

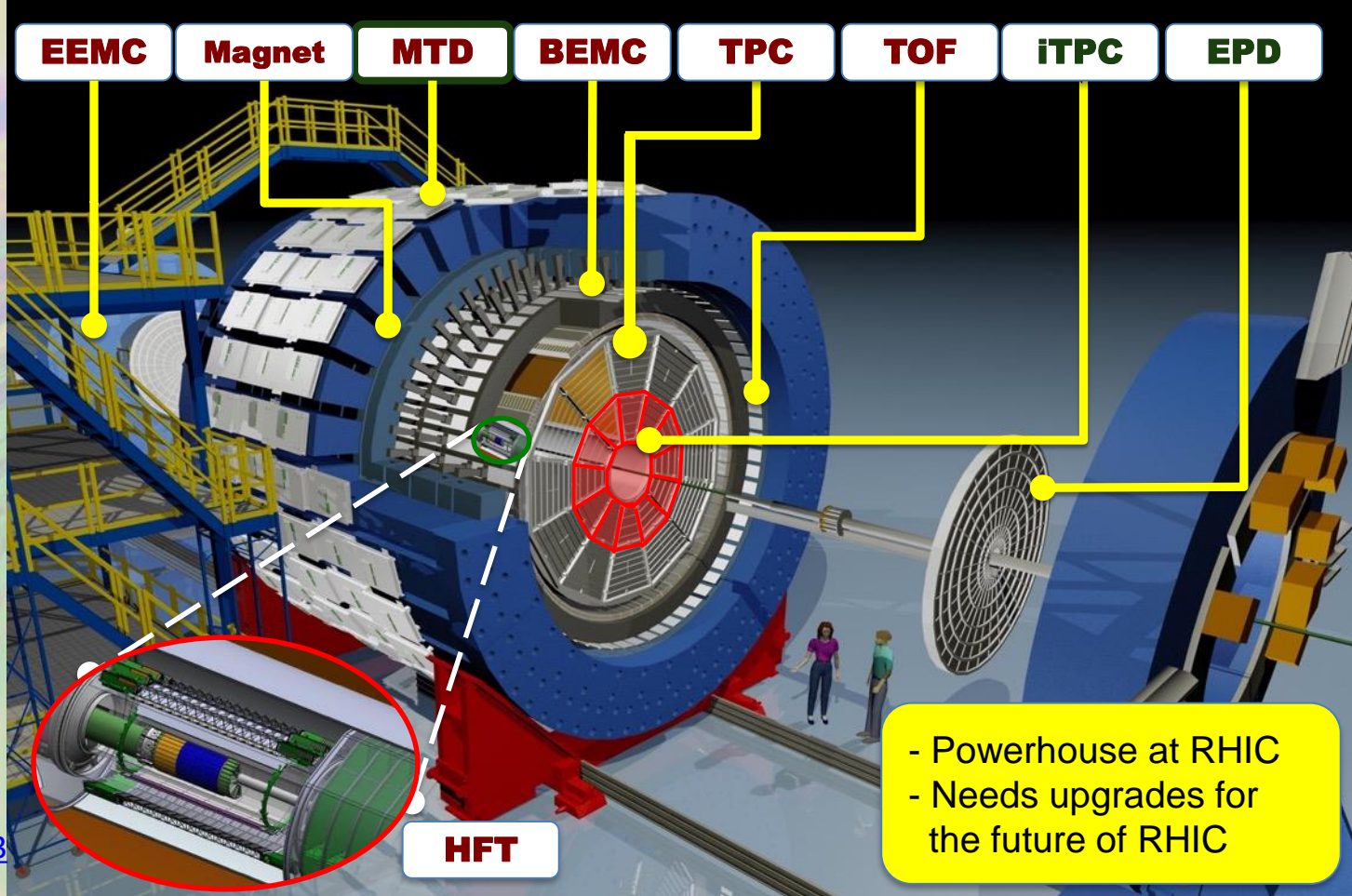
2022 – : RHIC+FAIR BES-III

Fixed-target programs

STAR Beam Energy Scan Program

- 1) Turn-off of sQGP signatures
- 2) Search for the signals of phase boundary
- 3) Search for the QCD critical point

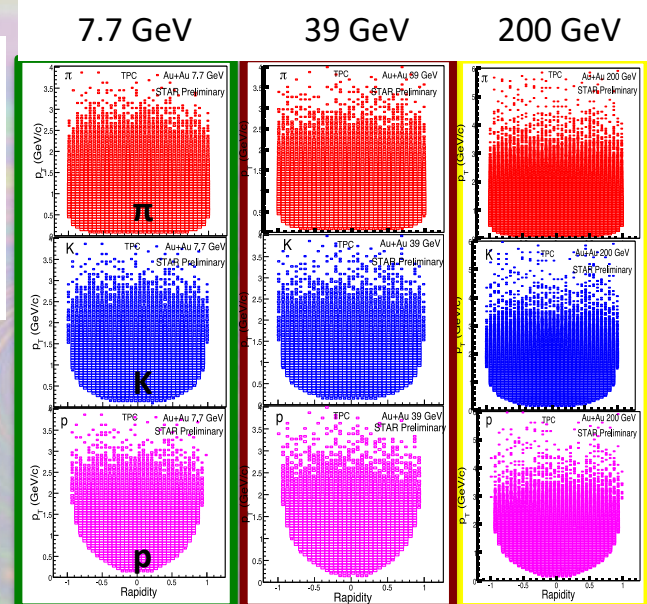
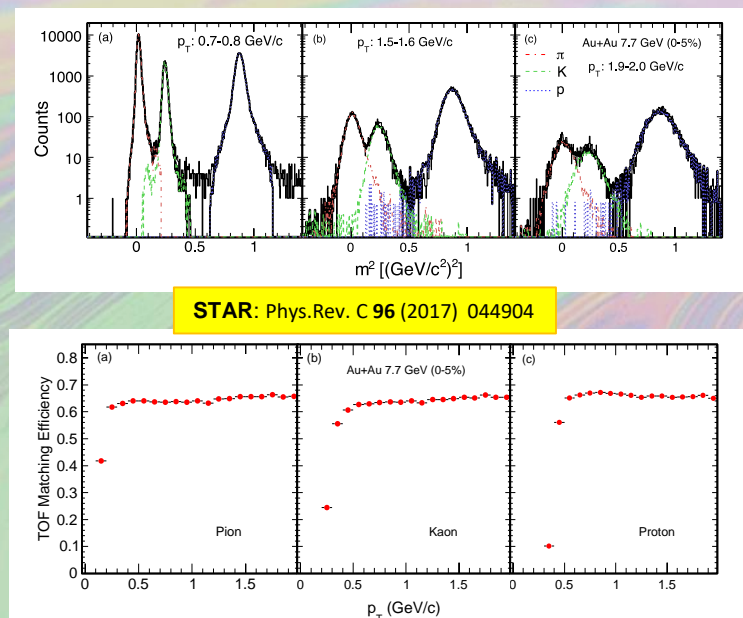
<http://arxiv.org/abs/1007.2613>



BES-I Au+Au Data Taking

Largest data sets versus collision energy!!!

$\sqrt{s_{NN}}$ [GeV]	events(10^6)	Year
200	350	2010
62.4	67	2010
54.4	300	2017
39	130	2010
27	70	2011
19.6	36	2011
14.5	20	2014
11.5	12	2010
7.7	5	2010
4.9 (FXT)	3.4	2015
4.5 (FXT)	1.3	2015



Geometric acceptance @ collider mode remains the same,
track density gets lower.
Detector performance generally improves at lower energies.

Excellent particle identification capabilities.
Large and homogeneous acceptance.
Especially important for fluctuation analysis

STAR publications on BES results

1. Inclusive charged hadron elliptic flow in Au + Au collisions at $\sqrt{s_{NN}} = 7.7\text{-}62.4 \text{ GeV}$, Phys. Rev. C **86** (2012) 54908
2. Observation of an energy-dependent difference in elliptic flow between particles and antiparticles in relativistic heavy ion collisions, Phys. Rev. Lett. **110** (2013) 142301
3. Elliptic flow of identified hadrons in Au+Au collisions at $\sqrt{s_{NN}} = 7.7\text{-}62.4 \text{ GeV}$, Phys. Rev. C **88** (2013) 14902
4. Energy Dependence of Moments of Net-proton Multiplicity Distributions at RHIC , Phys.Rev.Lett. **112** (2014) 032302
5. Beam-Energy Dependence of the Directed Flow of Protons, Antiprotons, and Pions in Au+Au Collisions , Phys.Rev.Lett. **112** (2014) 162301
6. Beam energy dependence of moments of the net-charge multiplicity distributions in Au+Au collisions at RHIC , Phys.Rev.Lett. **113** (2014) 092301
7. Beam-energy-dependent two-pion interferometry and the freeze-out eccentricity of pions measured in heavy ion collisions at the STAR detector , Phys.Rev. C **92** (2015) 014904
8. Energy dependence of acceptance-corrected dielectron excess mass spectrum at mid-rapidity in Au+Au collisions at $\sqrt{s_{NN}} = 19.6 \text{ and } 200 \text{ GeV}$, Phys.Lett. B **750** (2017) 64
9. Beam-energy dependence of charge separation along the magnetic field in Au+Au collisions at RHIC , Phys.Rev.Lett. **113** (2014) 052302

STAR publications on BES results

10. Energy Dependence of K/π , p/π , and K/p Fluctuations in Au+Au Collisions from $\sqrt{s_{NN}} = 7.7$ to 200 GeV , Phys.Rev. C **92** (2015) 021901
11. Observation of charge asymmetry dependence of pion elliptic flow and the possible chiral magnetic wave in heavy-ion collisions , Phys.Rev.Lett. **114** (2015) 252302
12. Probing parton dynamics of QCD matter with Ω and φ production, Phys.Rev. C **93** (2016) 021903
13. Beam-energy dependence of charge balance functions from Au + Au collisions at energies available at the BNL Relativistic Heavy Ion Collider , Phys.Rev. C **94** (2016) 024909
14. Centrality dependence of identified particle elliptic flow in relativistic heavy ion collisions at $\sqrt{s_{NN}}=7.7\text{--}62.4$ GeV , Phys.Rev. C **93** (2016) 014907
15. Beam Energy Dependence of the Third Harmonic of Azimuthal Correlations in Au+Au Collisions at RHIC , Phys.Rev.Lett. **116** (2016) 112302
16. Measurement of elliptic flow of light nuclei at $\sqrt{s_{NN}}= 200, 62.4, 39, 27, 19.6, 11.5$, and 7.7 GeV at the BNL Relativistic Heavy Ion Collider, Phys.Rev. C **94** (2016) 034908
17. Energy dependence of J/ψ production in Au+Au collisions at $\sqrt{s_{NN}}= 39, 62.4$ and 200 GeV, Phys.Lett. B **771** (2017) 13
18. Harmonic decomposition of three-particle azimuthal correlations at RHIC, arXiv:1701.06496

STAR publications on BES results

18. Global Λ hyperon polarization in nuclear collisions: evidence for the most vortical fluid, *Nature* 548, 62 (2017)
19. Bulk Properties of the Medium Produced in Relativistic Heavy-Ion Collisions from the Beam Energy Scan Program, *Phys.Rev. C* 96 (2017) 044904
21. Beam Energy Dependence of Jet-Quenching Effects in Au+Au Collisions at $\sqrt{s_{NN}} = 7.7, 11.5, 14.5, 19.6, 27, 39$, and 62.4 GeV , arXiv:1707.01988
22. Beam-Energy Dependence of Directed Flow of Λ , anti Λ , K^\pm , K_s^0 and φ in Au+Au Collisions, arXiv:1708.07132, accepted to *Phys.Rev.Lett.*
23. Collision Energy Dependence of Moments of Net-Kaon Multiplicity Distributions at RHIC, arXiv:1709.00773

1 Nature + 8 PRL + 2 PLB + 9 PRC

+ many conference proceedings...



Isaac Upsal, OSU

The STAR Collaboration

The image shows the front cover of the magazine 'nature'. The title 'nature' is written in a large, blue, serif font at the top. Below it, in a smaller white font, is the subtitle 'THE INTERNATIONAL WEEKLY JOURNAL OF SCIENCE'. The central visual element is a circular diagram composed of numerous thin, light-blue lines radiating from a central point, resembling the tracks left by particles in a detector. A small black circle is positioned in the center of this pattern, containing the text 'First observation of fluid vortices formed by heavy-ion collisions' in white, followed by 'PAGES 34 & 62' in a smaller font. At the bottom of the cover, the word 'SUBATOMIC SWIRL' is printed in large, bold, white, sans-serif letters.



Mike Lisa, OSU



Sergej Voloshin, WSU

LIVE SCIENCE
NEWS TECH HEALTH PLANET EARTH STI
Live Science • Strange News

Objev nejrychleji rotující kapaliny může vést k pochopení vzniku vesmíru

Čeští vědci z Ústavu jaderné fyziky Akademie věd ČR a pražského ČVUT společně s kolegy z dalších 12 zemí prokázali, že kvark-gluonové pláze je tektinou s největší stranou publikoval prestižní časopis Nature. Význam objevu umožní věsmírné hmoty krátce po velkém třesku, uvedl Michal Šumbera

World's Fastest-Swirling Vortex Simulates the Big Bang

ars TECHNICA
SPIN CITY — Taking quark-gluon plasma for a spin may un-break a fundamental symmetry

Their rotations may tell us fundamental things about quantum chromodynamics.

EurekAlert! The Global Source for Science News AAAS

HOME NEWS MULTIMEDIA MEETINGS PORTALS

PUBLIC RELEASE: 2-AUG-2017

'Perfect liquid' quark-gluon plasma is the most vortical fluid

The Telegraph India
Wednesday, August 9, 2017

PHYS.ORG Nanotechnology Physics Earth Astronomy & Space Technology Chemistry

Fluid spins trillions of times faster than

ScienceDaily Your source for the latest research news

夸克胶子等离子体“整体极化”理论获证

最新发现与创新

科技日报济南8月3日电 (记者王延斌 通讯员车慧卿)宇宙在最初诞生百万分之几秒内以“夸克胶子等离子体”的形式存在，这种类似“电浆”的状态是固体、液体、气体之后的第四种物质形态。近日，我国科学家首次提出的

DOE SCIENCE NEWS SOURCE

ScienceNews MISSION CRITICAL Support credible science journalism. Subscribe to Science News today!

Smashing gold ions creates most swirly fluid ever

Record-making vortex found in quark-gluon plasma

CERN COURIER INTERNATIONAL JOURNAL OF HIGH-ENERGY PHYSICS

Volume 67 Number 8 December 2017

HEAVY IONS
Fastest spinning fluid clocked by RHIC

Experiments at the Relativistic Heavy Ion Collider (RHIC) at Brookhaven National Laboratory have found that droplets of quark-gluon plasma (QGP) can spin faster than any other fluid. The immensely hot and fast-expanding QGP is already known to behave as near “perfect” liquid, exhibiting a viscosity lower than any other. Now, researchers on RHIC’s STAR experiment report that the vorticity (or curl) of the fluid produced in RHIC’s relativistic heavy-ion collisions is about 9×10^8 s⁻¹. That exceeds

newsR Edition: India

HOME NATIONAL WORLD SPORTS POLITICS BUSINESS PEOPLE

+ Science + Technology Computer Industry

Facebook Page CURRENT TOPICS

Pulwama Tal Afar Typhoon Hato Moin Qureshi Hurricane Harvey SPOTLIGHT Live TV Movie Reviews

Perfect liquid quark-gluon plasma is the most vortical fluid

ENERGY DAILY Friday, 4 August 2017 (22 days ago)

Upton, NY (SPX) Aug 03, 2017

Particle collisions recreating the quark-gluon plasma (QGP) that filled the early universe reveal that droplets of this primordial soup swirl far faster than any other fluid. The new analysis of data from the Relativistic Heavy Ion Collider (RHIC) - a U.S. Department of Energy Office of Science User Facility for nuclear physics research at Brookhaven National Laboratory - shows that the

Spektrum.de SUCHEN Magazine | Archiv | Shop/Artikel

Gehim & Seele

Der schnellste Wirbel des Universums?

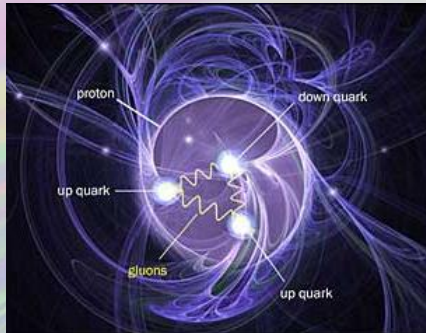
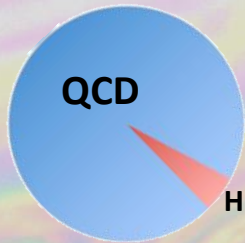
Den schnellsten bisher gemessenen Wirbel erzeugten Physiker in einem Teilchenbeschleuniger. Die Flüssigkeit ist dabei ein Plasma aus fundamentalen Teilchen: Quarks und Gluonen.

von Manon Bischoff

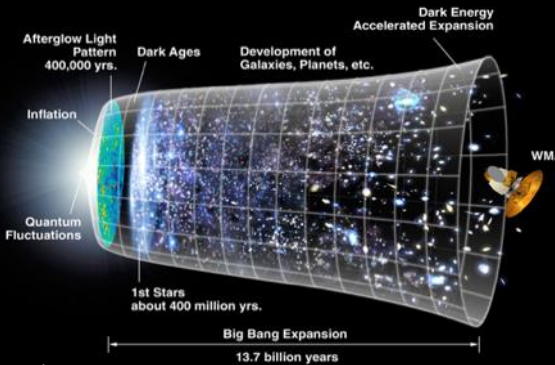
GIVING IT A WHIRL. Colliding gold ions in the STAR experiment create an intensely whirling fluid. The mass of particles emitted in each collision like the ones shown above kilometers below ground, the earth.

© Poltyakov / Getty Images / iStock (Auschnitt)

What we're after*



The Universe



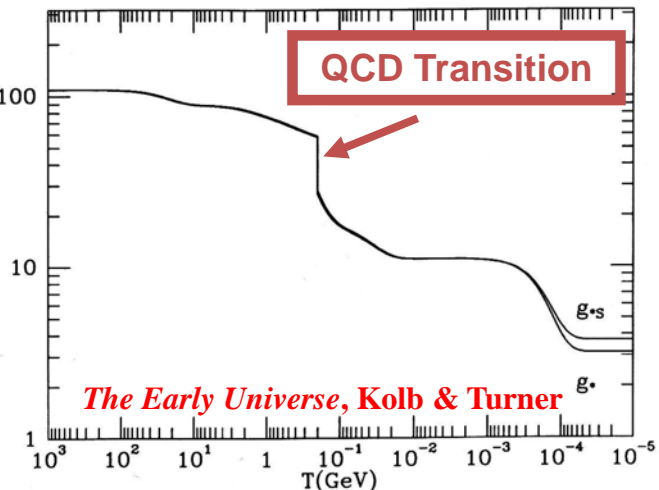
Credit: NASA

Fundamental understanding of the Strong Interaction

- confines color
- generates ~95% of visible mass

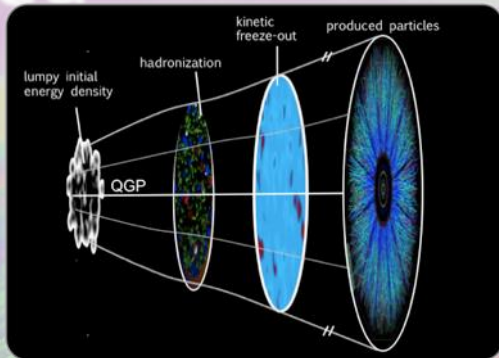
*) Many references, including those to other reviews can be found in R. Pasechnik, M. Šumbera: Phenomenological Review on Quark–Gluon Plasma: Concepts vs. Observations, Universe 3 (2017) no.1, 7, arXiv:1611.01533

Thermodynamic degeneracy

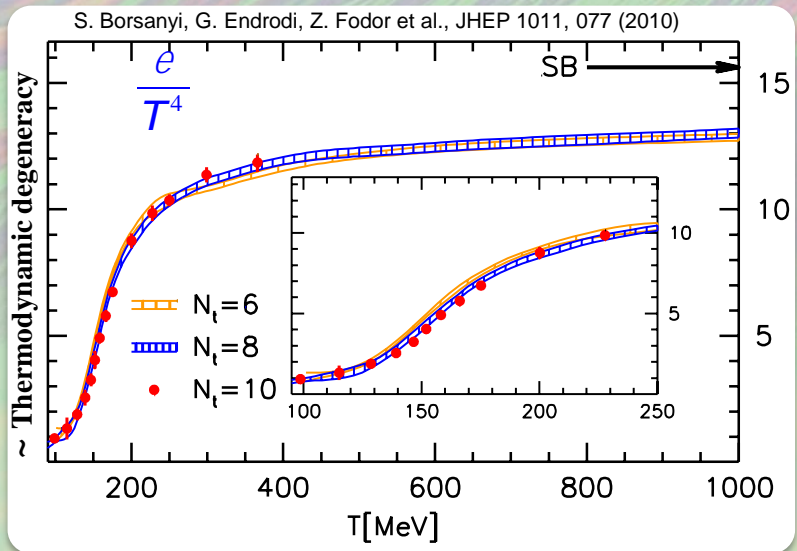
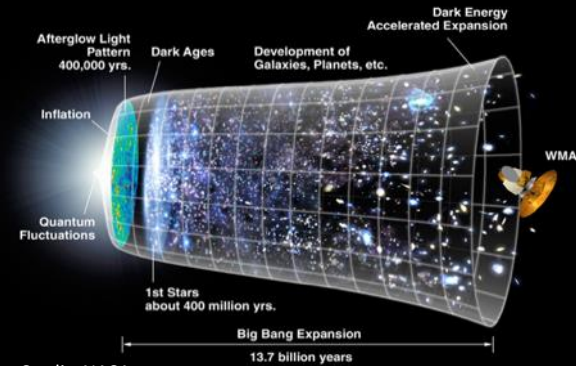


What we expected

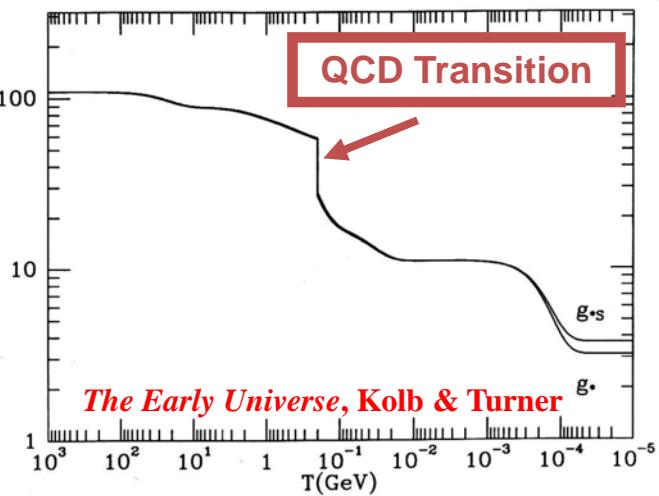
Lattice QCD:
weakly-interacting parton gas



The Universe



Thermodynamic degeneracy



What we found



New State of Matter Is 'Nearly Perfect' Liquid

Physicists working at Brookhaven National Laboratory announced today that they have created what appears to be a new state of matter out of the building blocks of atomic nuclei, quarks and gluons. The researchers unveiled their findings—which could provide new insight into the composition of the universe just moments after the big bang—today in Florida at a meeting of the American Physical Society.

SCIENTIFIC AMERICAN



Lattice QCD:

- The lattice calculations were not wrong. Our physical understanding based on them was wrong (weakly vs strongly coupled).
 - detailed experimental probes dislodged our misconceptions
- Hydro treatment is now a crucial element of H.I.C. Standard Model*
 - Access to Equation of State, transport coefficients, time evolution
- We must continue to subject our new paradigm to detailed experimental scrutiny
- Even assuming hydro: Do we sufficiently understand the fluid structure?

Edward Shuryak, *Strongly coupled quark-gluon plasma in heavy ion collisions*, Rev.Mod.Phys. 89 (2017) 03500



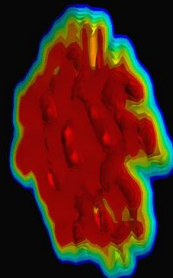
Associated Press
Tuesday, April 19, 2005, Page A05
The Washington Post

The universe behaved like a liquid in its earliest moments, not the fiery gas that was thought to have pervaded the first microseconds of existence.

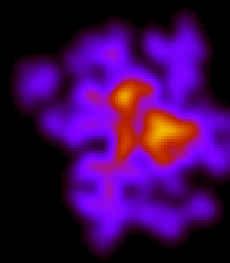
*) All hard hadronic process are strongly quenched, all soft particles emerge from the common flow field

Hydrodynamics – standard paradigm of H.I.C

movies by Bjorn Schenke



$t = 0.5 \text{ fm}/c$



Modern approach*:

Fluid dynamics is a long-wavelength effective theory based on knowledge of the effective degrees of freedom, and the symmetries of the system under consideration.

From a (lumpy) initial state, solve hydro equations:

$$\partial_\mu T^{\mu\nu} = 0; \quad T^{\mu\nu} = \epsilon u^\mu u^\nu - (p + \Pi) \Delta^{\mu\nu} + \pi^{\mu\nu}$$

$$\Delta^{\mu\nu} = g^{\mu\nu} - u^\mu u^\nu; \quad \epsilon = u^\mu T^{\mu\nu} u^\nu$$

$$p = p_s + \Pi = -\frac{1}{3} \Delta_{\mu\nu} T^{\mu\nu}; \quad \Pi = -\zeta \partial_\mu u^\mu$$

$$u^\mu \partial_\mu \Pi = \frac{1}{\tau_\Pi} (\Pi + \zeta \theta) - \frac{1}{2} \Pi \frac{\zeta_T}{\tau_\Pi} \partial_\mu \left(\frac{\tau_\Pi}{\zeta_T} u^\mu \right)$$

& many more terms...

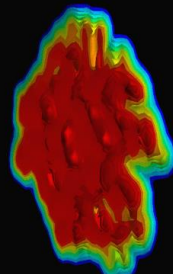
N.B. For Bjorken flow $u^\mu = x^\mu / \tau$:

$$\frac{d\epsilon}{d\tau} = -\frac{\epsilon + p_s}{\tau} \left(1 - \frac{4}{\tau T} \frac{\eta}{s} - \frac{1}{\tau T} \frac{\zeta}{s} \right)$$

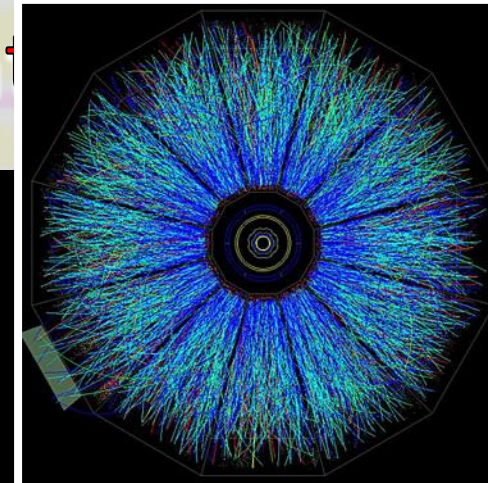
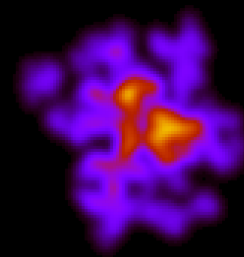
*) For recent reviews of new theories of relativistic hydrodynamics see:
P. Romatschke, U. Romatschke, arXiv:1712.05815
W. Florkowski, M.P. Heller and M. Spalinski, arXiv:1707.02282

Connection to experiment

movies by Bjorn Schenke

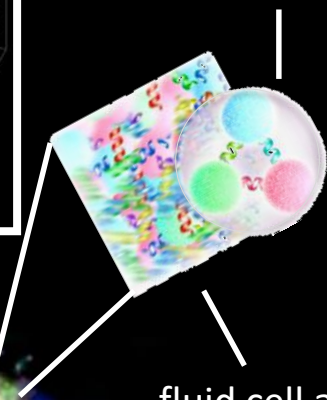


$t = 0.5 \text{ fm/c}$

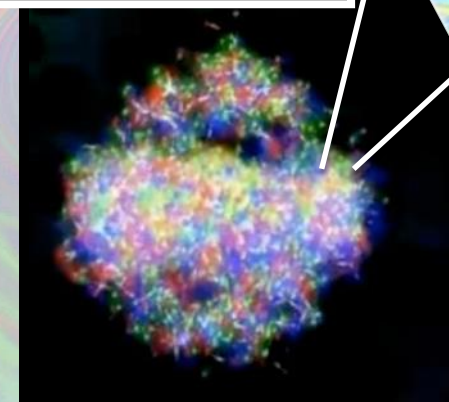


t

emitted hadron
(color confined)



fluid cell at
freeze-out



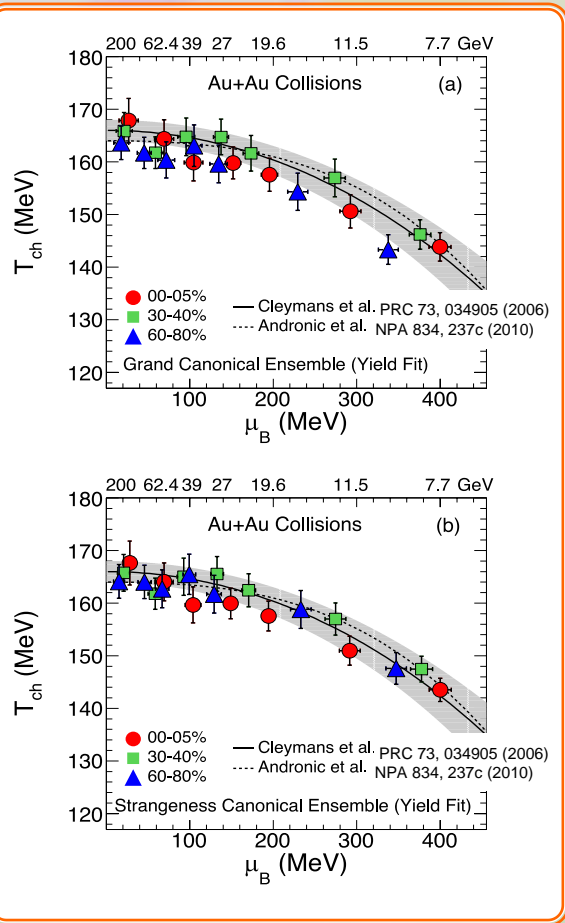
QGP fluid:
colored quarks deconfined

System cools & expands \rightarrow Freeze-out

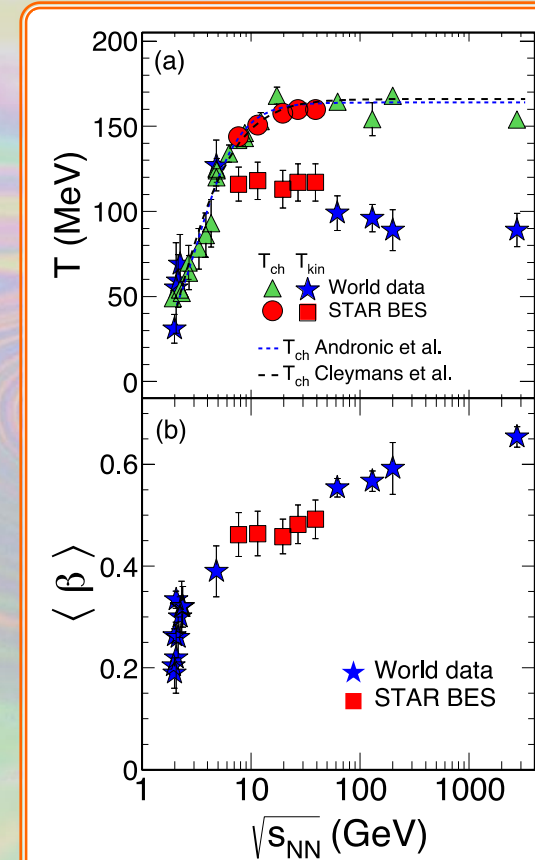
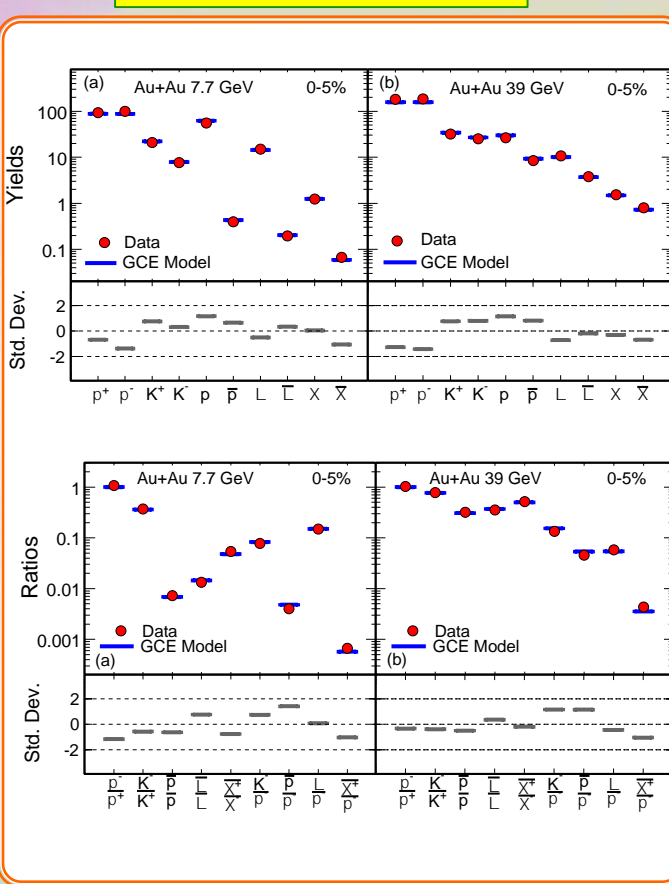
- Cooper-Frye prescription* – “physics-free”.
- Emited hadrons reflect properties of their parent hydro cell (chemical potentials, thermal and collective velocities).

$$*) E \frac{d^3 N}{d^3 p} = \frac{g}{(2\pi)^3} \int e^{-(u^\nu p_\nu - \mu)/T_{kin}} p^\lambda d\sigma_\lambda$$

Bulk Properties at Freeze-out and Statistical Hadronization Models

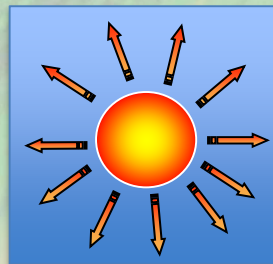
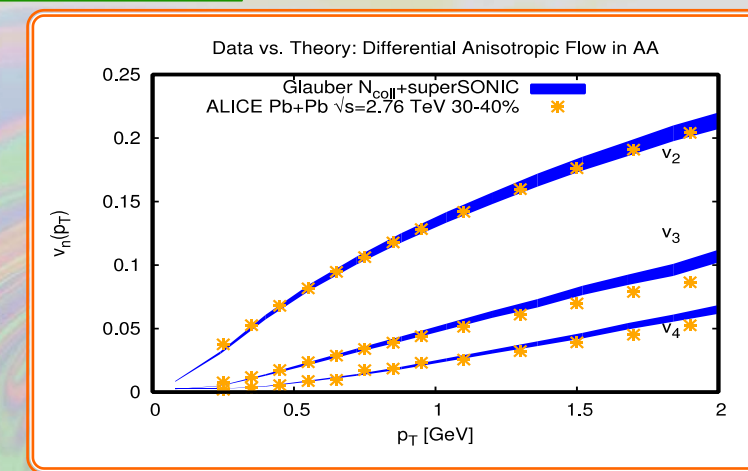
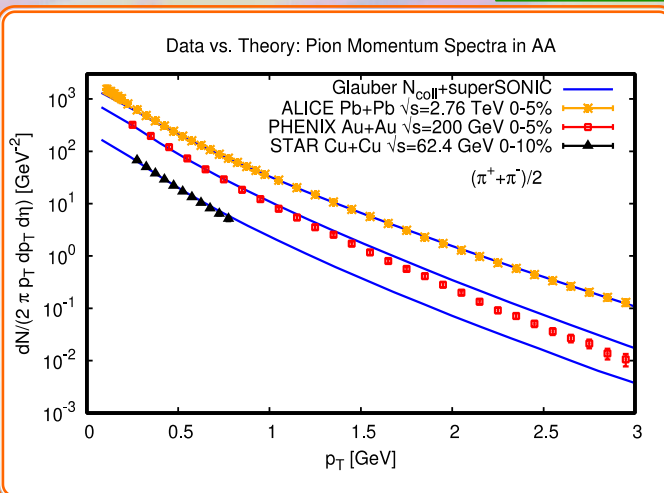


STAR: Phys.Rev. C 96 (2017) 044904

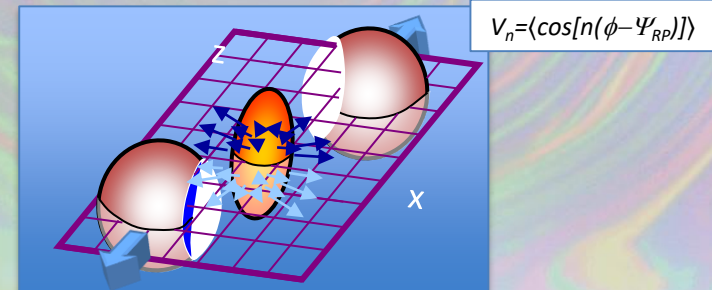


Hydro works for A+A collisions at RHIC and LHC

P. Romatschke, U. Romatschke, arXiv:1712.05815



Radial Flow

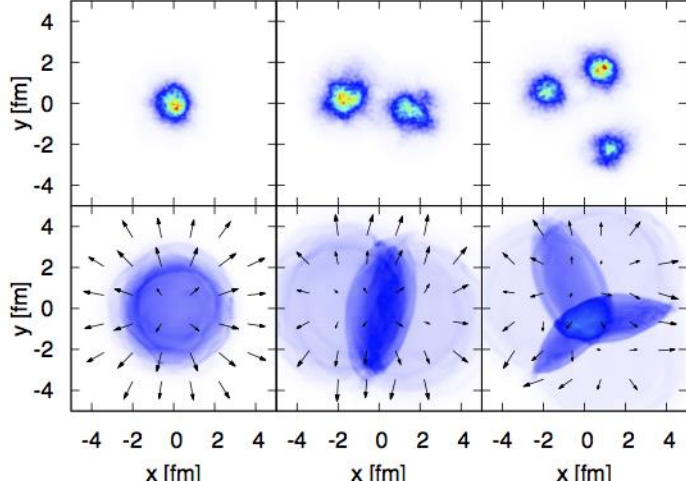


Elliptic Flow

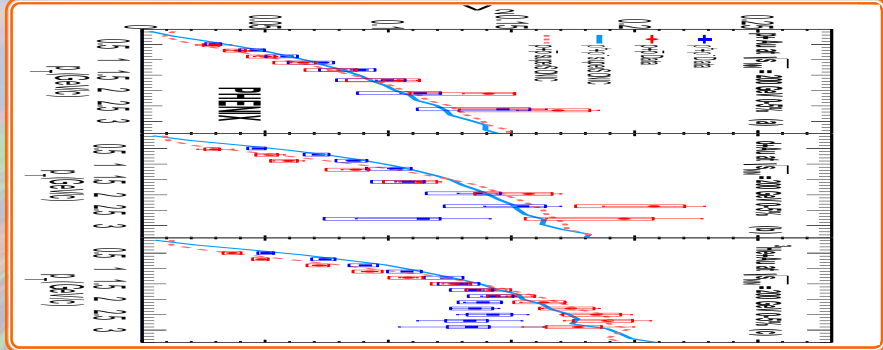
..and for (p,d, ^3He)+Au at RHIC!!!

B. Schenke, Nucl.Phys. A967(2017)105

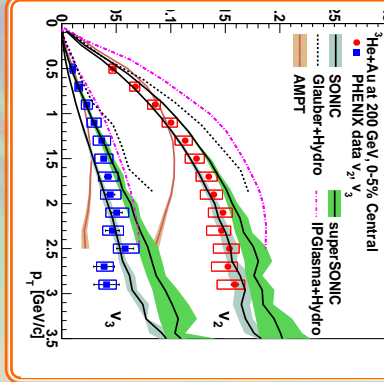
p+Au d+Au $^3\text{He}+\text{Au}$



PHENIX, arXiv:1710.09736



PHENIX, Phys.Rev.Lett. 115 (2015)142301

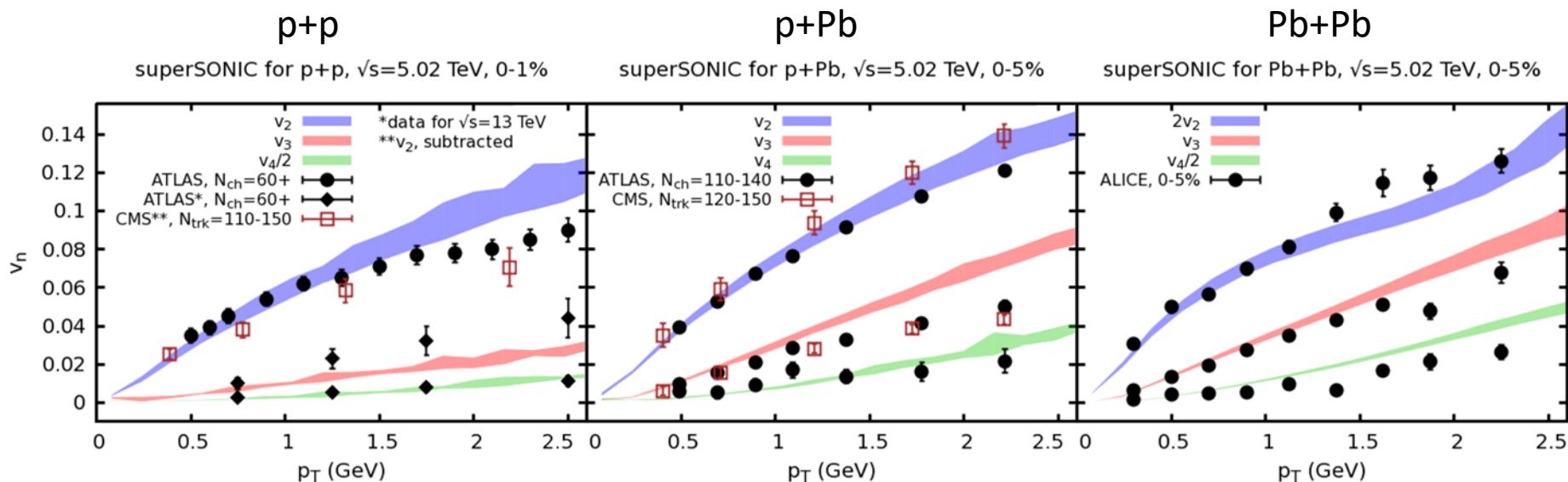


$$V_n = \langle \cos[n(\phi - \Psi_{RP})] \rangle$$

sQGP \Rightarrow FSI dominates momentum space correlations \Rightarrow final state is very sensitive to the initial shape of the collision system.
 \Rightarrow Using varying small projectiles (p, d, or ^3He) to modify the average geometry one expects modification of the measured ellipticity and triangularity coefficients v_2 and v_3 .

... and even for high-multiplicity p+p events at LHC !!!

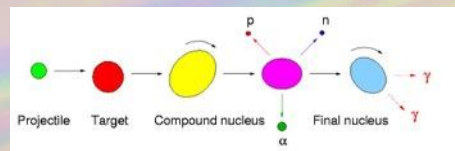
R.D. Weller, P. Romatschke, Phys.Lett. B 774 (2017) 351



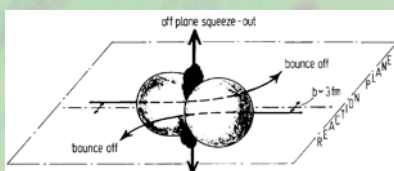
Using initial conditions that allow for nucleon substructure in the form of three valence quarks all collision systems can be described simultaneously with a single set of fluid parameters.

Developing a finer probe/test of hydro

$V_2 > 0$: (rotating) compound nucleus formation



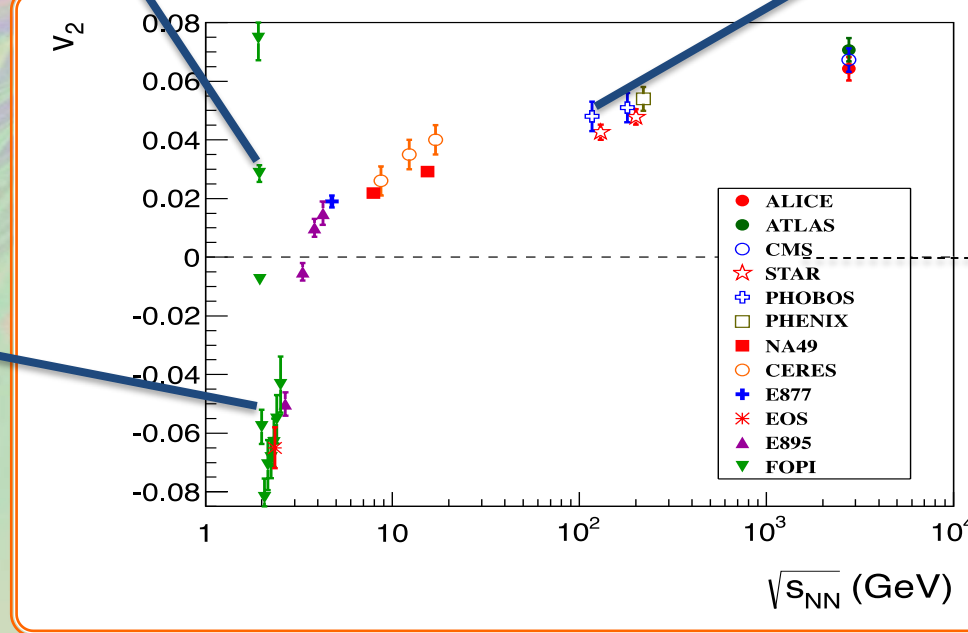
$V_2 < 0$: shadowing by spectators (squeeze-out)



$V_2 > 0$: strongly interacting matter

$V_2 > 0$: in-plane

$V_2 < 0$: out-of-plane

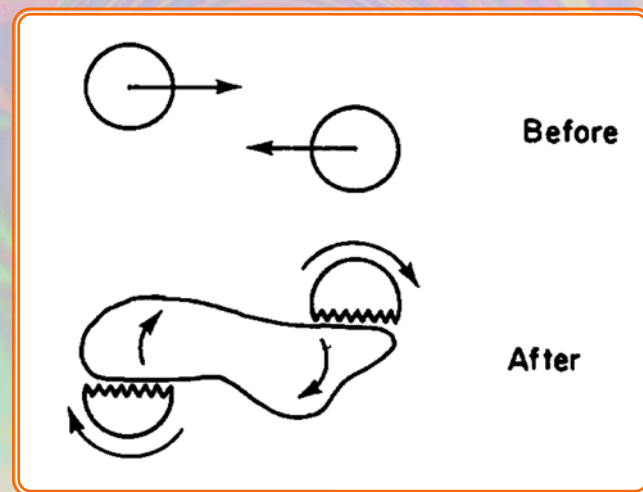


Developing a finer probe/test of hydro

- Non-central heavy ion collisions: $J \sim 10^5 \hbar \approx N_{\text{part}} \times (v s_{\text{NN}}/2) \times b$
- N.B. Calculations behind the “perfect fluid” story neglect angular momentum altogether.
- Effect on hydrodynamic system?
- What is the experimental probe?

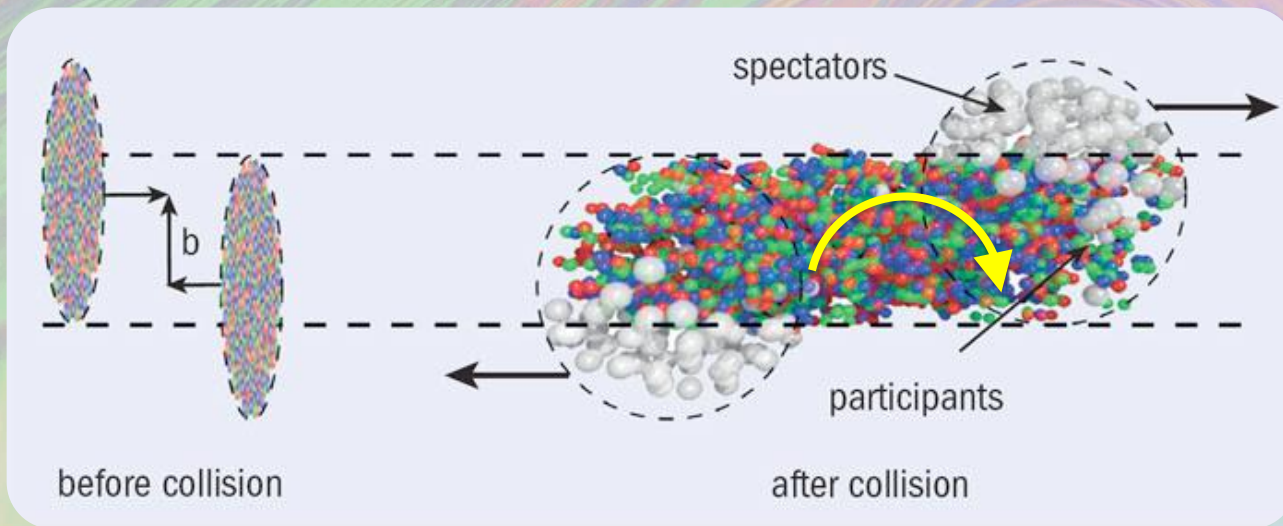
P. Carruthers, Nuclear Physic A 418(1984)501c – Proc. Quark Matter II

...note that if the excitations are energized in a nucleus-nucleus collision, considerable angular momentum is likely to be concentrated in vorticle eddies, which could decay as coherent blasts of vector particles ...



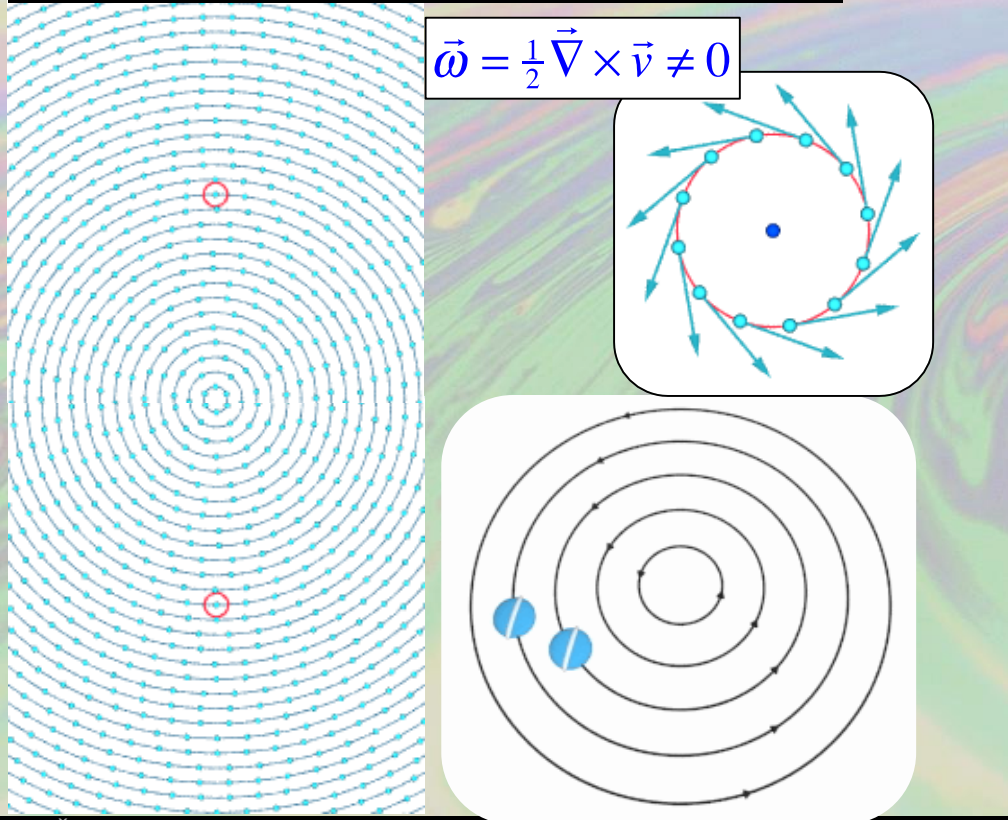
A finer probe?

- Non-central collision: $J \sim 10^5 \hbar$
- In a hydrodynamic picture, relevant quantity is vorticity $\vec{\omega} = \frac{1}{2} \vec{\nabla} \times \vec{v}$
- How would this manifest experimentally?

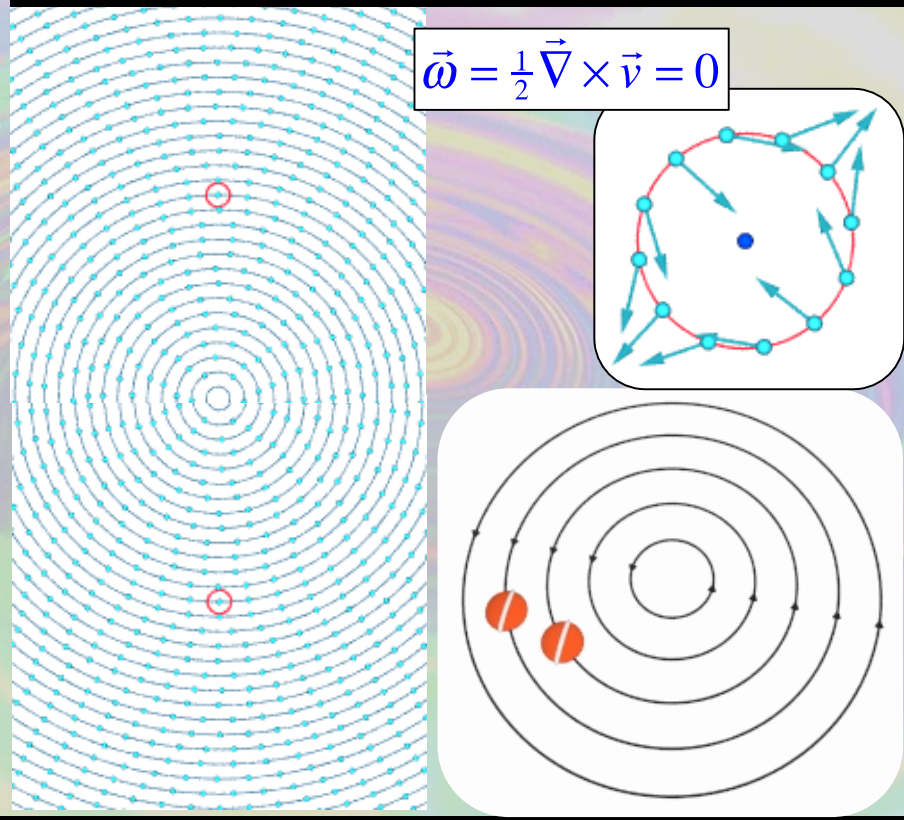


Rotational & irrotational vortices

Rotational Vortex (e.g. rigid body): $V \propto r$



Irrational Vortex (e.g. tub drain): $V \propto 1/r$



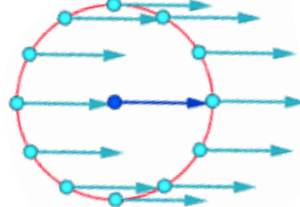
Shear field vorticity

Localized vortex generation via baryon stopping

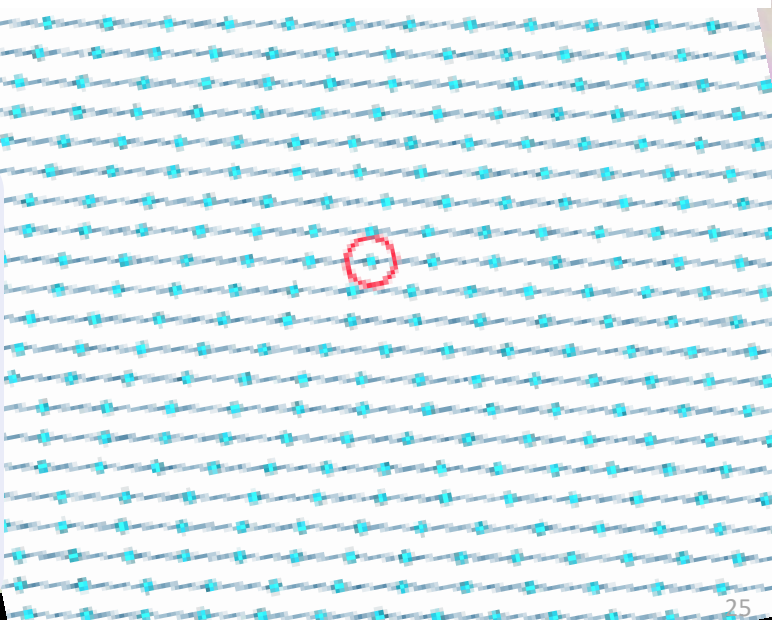
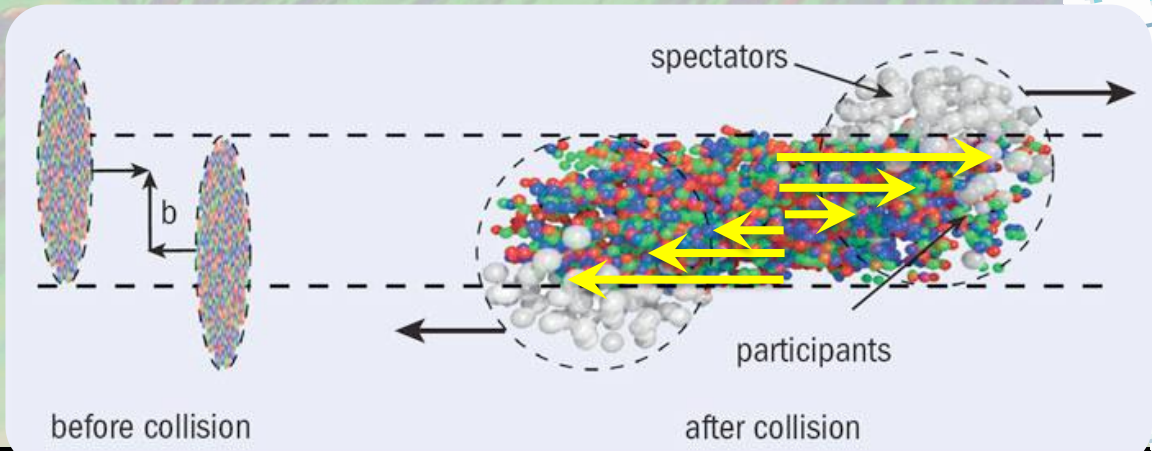
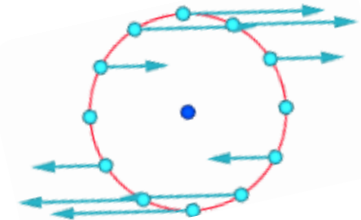
Viscosity dissipates vorticity to fluid at larger scale

More natural structure for plasma
from nuclear collision: $\omega = \frac{1}{2} \nabla \times \vec{v} \approx \frac{1}{2} \frac{\partial v_z}{\partial x}$

In collision c.m. frame



In local frame of fluid cell



Heavy ion collisions – source of the strongest magnetic fields

Biot-Savart law:

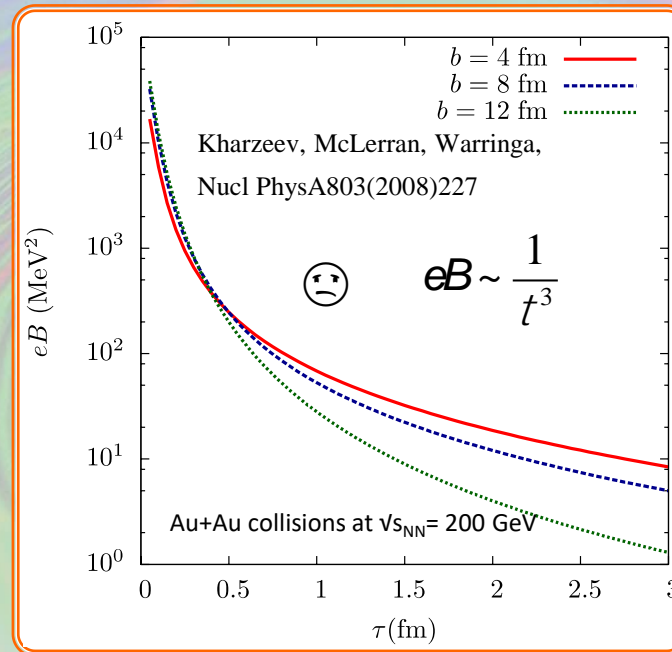
$$B \gg g Z e \frac{b}{R_A^3}$$

$$g = \sqrt{s_{NN}} / 2m_N$$

$$g = 100, Z = 79,$$

$$b \gg R_A = 7\text{ fm}$$

$$\Rightarrow eB \gg m_p^2 \sim 10^{18} \text{ Gauss}$$

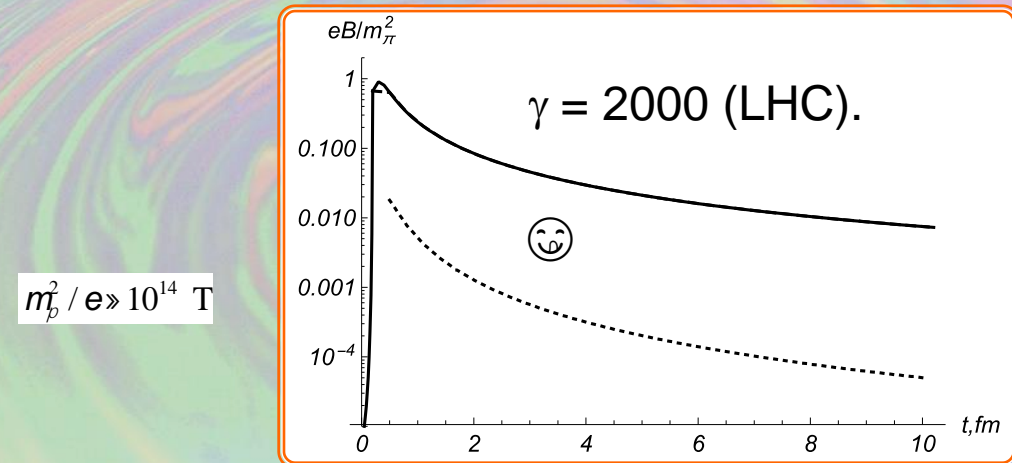
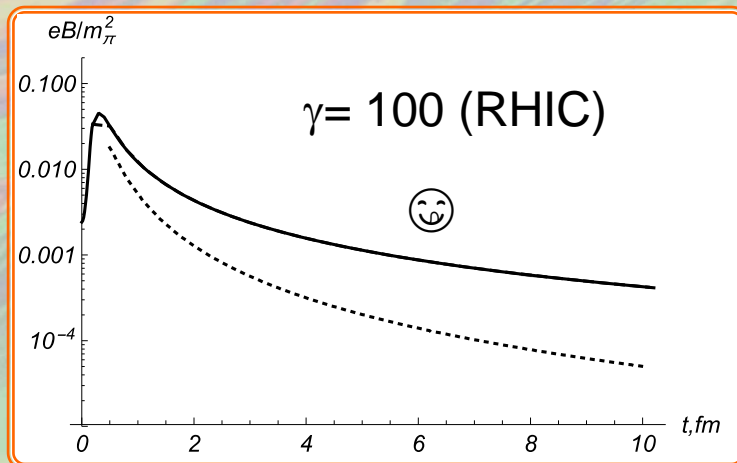


Magnetic field evolution in the presence of QGP medium

The time-evolution and the strength of magnetic field are strongly affected by the electrical conductivity $\sigma(t)$ of the plasma.

$$\sigma(t) = \frac{\sigma}{2^{-1/3}(1 + t/t_0)^{1/3}}$$

K. Tuchin: Phys.Rev. C93 (2016) no.1, 014905



$$m_p^2 / e \gg 10^{14} \text{ T}$$

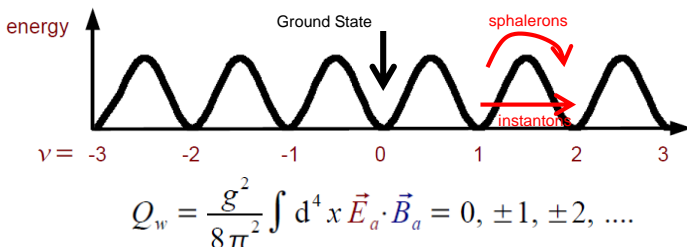
Magnetic field in units of m_π^2/e . $\sigma = 5.8 \text{ MeV}$, $z = 0.2 \text{ fm}$, $t_0 = 0.2 \text{ fm}$. Solid, dashed and dotted lines stand for B , B_{init} and B_{val} .

Hot QCD allows for metastable states

... lots of them

D.E. Kharzeev *et al.* Prog. Part. Nucl. Phys. 88 (2016) 1

QCD has an infinite number of vacua which can distinguished by a winding number $\nu = 0, \pm 1, \pm 2, \dots$



$$Q_w = \frac{g^2}{8\pi^2} \int d^4x \vec{E}_a \cdot \vec{B}_a = 0, \pm 1, \pm 2, \dots$$

In chiral limit ($m=0$): $[N_L - N_R]_{t=\infty} - [N_L - N_R]_{t=-\infty} = 2N_f Q_w$

Kharzeev, McLellan, and Warringa arXiv:0711.0950 and Nucl. Phys. A803 (2008) 227:

“The consequences and magnitude of these effects are subject to experimental study and verification”

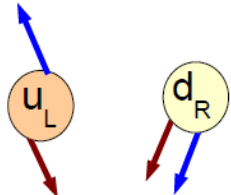
- Gauge theories with compact symmetry groups possess topologically nontrivial configurations of gauge field.
- Dramatic implications for the vacuum structure of QCD at high T^* .
- Moving from one vacuum state to another results in changing the topological charge Q_w of the system.
- Q_w flips helicity and thus counts the difference between the number of right and left handed quarks.
- Q_w changing transitions also violate local P and CP conservation.

*) N.B. deconfinement transition is accompanied by a rapid change in the rate and nature of topological transitions connecting different topological sectors.

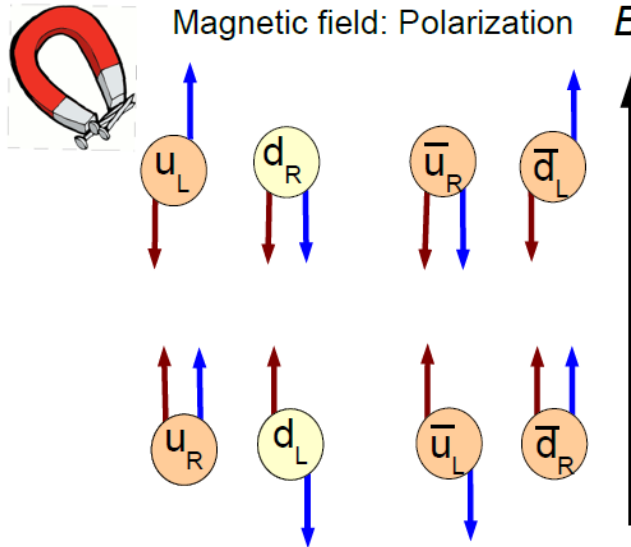
How does the B field affect the (massless) quarks

A magnetic field will align the spins, depending on their electric charge

No Magnetic Field: No polarization



Magnetic field: Polarization B



The momenta of the quarks align along the magnetic field

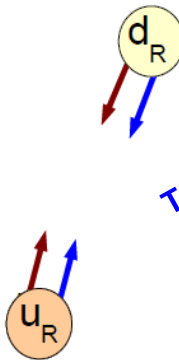
A quark with right-handed helicity will have momentum opposite to a left-handed one

In this way the magnetic field can distinguish between right and left

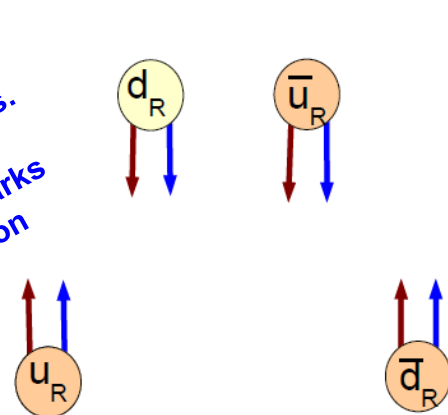
Topological charge flips chirality: L to R

A magnetic field will align the spins, depending on their electric charge

No Magnetic Field: No polarization



Magnetic field: Polarization B



Topological Charge fluctuations create an excess of right, or left handed quarks.
Note that right handed quarks move up or down based on charge.

Positively charged particles move parallel the magnetic field

Negatively charged particles move to antiparallel to magnetic field

An electromagnetic current is created along the magnetic field

Observing Topological Charge Transition

To observe in the lab

- add massless fermions (chiral quarks and anti-quarks)
- apply a magnetic field

CME task force report: arXiv: 1608.00982

A required set of Extraordinary Phenomena:

QCD Topological Charge + Chiral Symmetry Restoration
+ Strong Magnetic Field \Rightarrow **Chiral Magnetic Effect** =
QCD anomaly driven chirality imbalance leading to
current along B-field

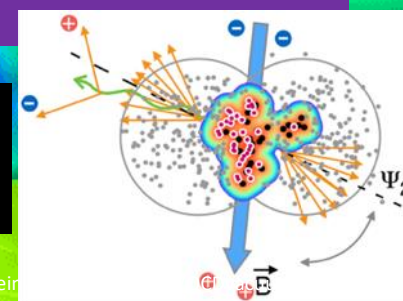
Observable:

Chirally restored quarks separated
along magnetic field

Experimental strategy:

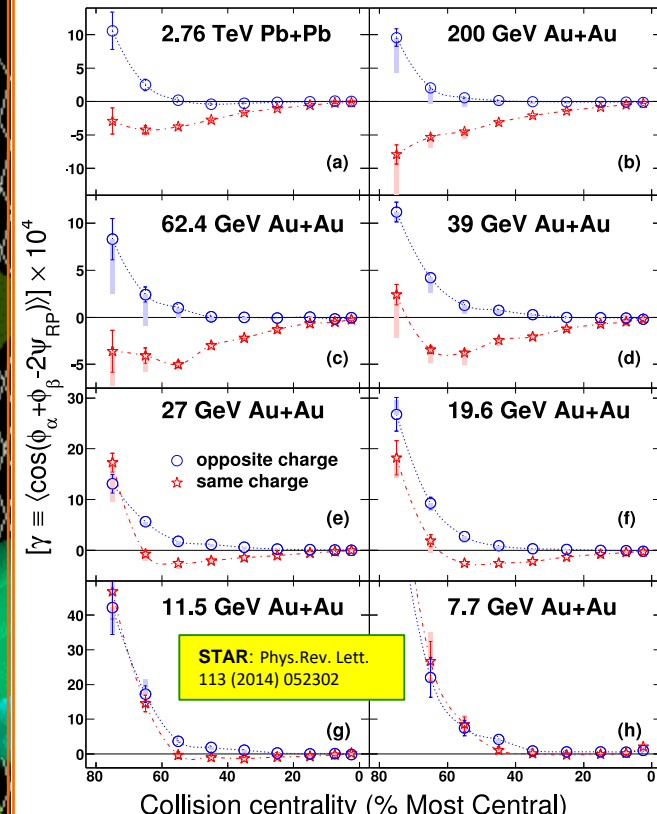
Measure 2 particle correlations
 $(++, --, + -)$ WRT reaction plane

<http://www.physics.adelaide.edu.au/theory/staff/leir>



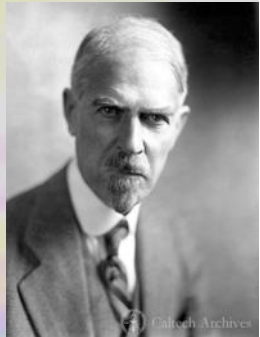
36cool30action.gif

Charge separation 7.7-2760 GeV



Necessary but not sufficient condition for
the CME (other explanation not ruled out)

One year, two discoveries



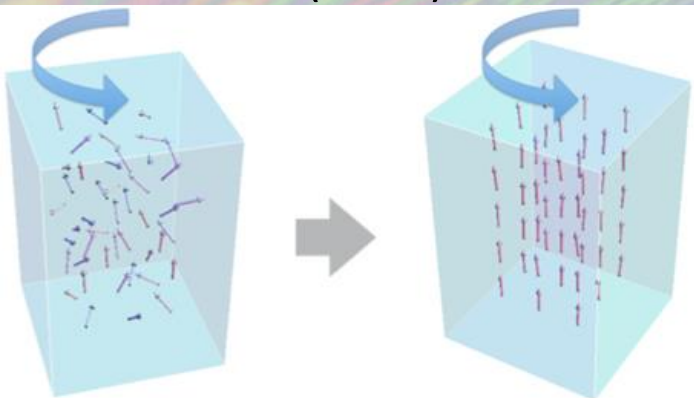
THE
PHYSICAL REVIEW.

MAGNETIZATION BY ROTATION.¹

By S. J. BARNETT.

§1. In 1909 it occurred to me, while thinking about the origin of terrestrial magnetism, that a substance which is magnetic (and therefore, according to the ideas of Langevin and others, constituted of atomic or molecular orbital systems with individual magnetic moments fixed

Barnett Effect (1915)



$$\vec{B} = \vec{\omega}/\gamma$$

$$M = \chi \omega / \gamma$$

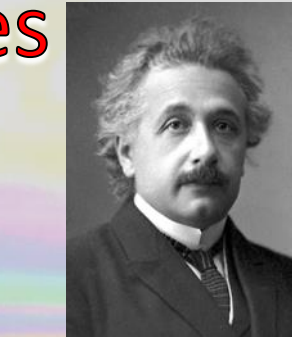
M – magnetization

γ – gyromagnetic ratio

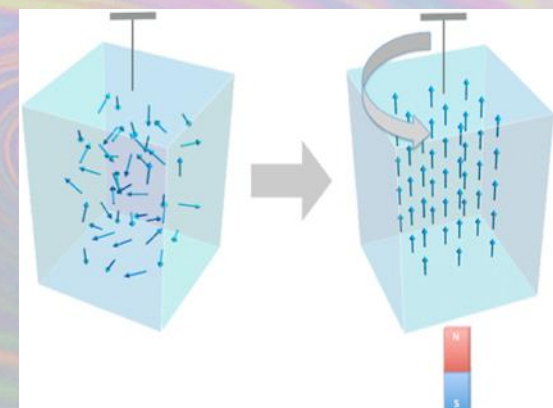
χ – magnetic susceptibility

S. J. Barnett, Rev. Mod. Phys. 7 (1935) 129

uncharged metal object:
mechanical rotation → magnetization



Einstein-de Haas Effect (1915)

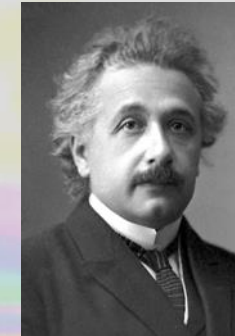


unmagnetized metal object:
introduce B-field → mechanical rotation



Einstein-de Haas Effect (1915)

This is the only experimental result Einstein published



696

Physics. — “*Experimental proof of the existence of Ampère's molecular currents.*” By Prof. A. EINSTEIN and Dr. W. J. DE HAAS.
(Communicated by Prof. H. A. LORENTZ),

(Communicated in the meeting of April 23, 1915).

When it had been discovered by OERSTED that magnetic actions are exerted not only by permanent magnets, but also by electric currents, there seemed to be two entirely different ways in which a magnetic field can be produced. This conception, however, could

(* N.B. electron spin discovered in 1925)

First observation of vorticity-polarization coupling

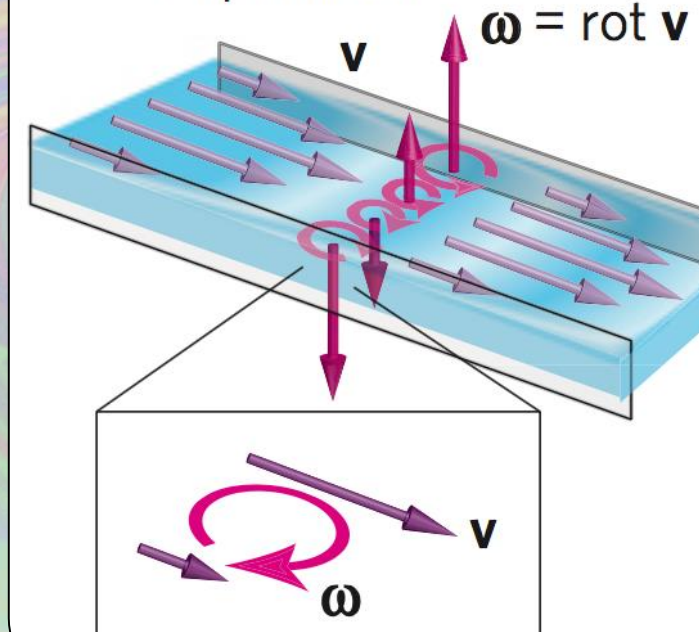
Takahashi, et al. : Spin hydrodynamic generation, *Nature Physics* 12, 52–56 (2016)

1. Hg flowing down a channel

- viscous forces with walls → fluid vorticity

1

Liquid flow

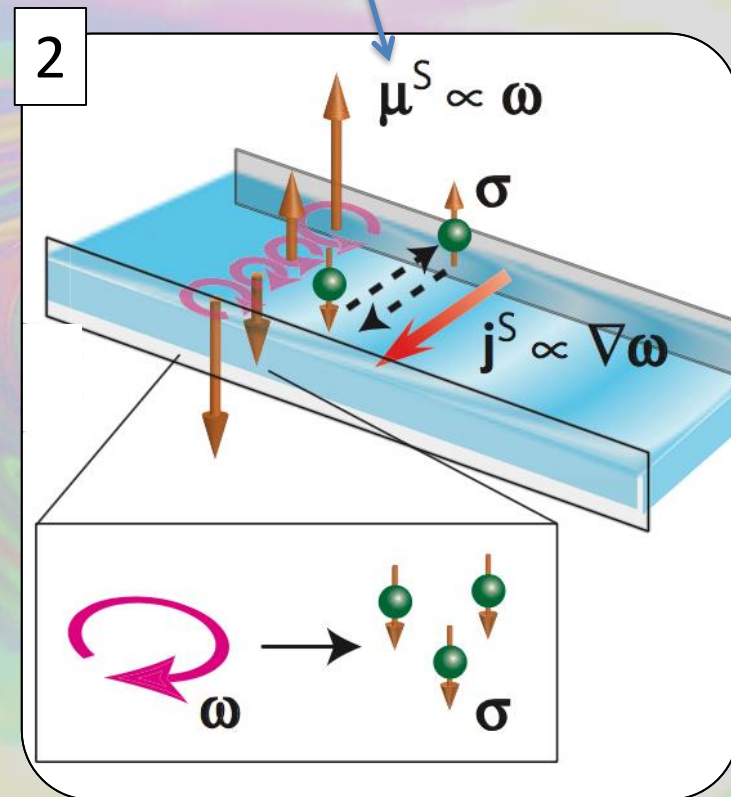


First observation of vorticity-polarization coupling

Takahashi, et al. : Spin hydrodynamic generation, *Nature Physics* 12, 52–56 (2016)

1. Hg flowing down a channel
 - viscous forces with walls \Rightarrow fluid vorticity
2. mechanical fluid vorticity \Rightarrow e^- polarization

μ^S = spin chemical potential



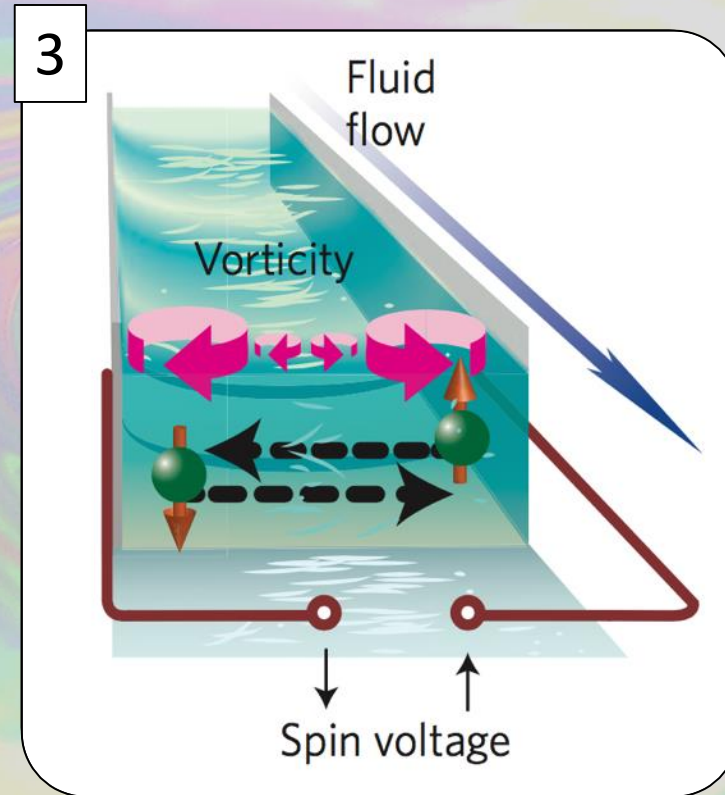
First observation of vorticity-polarization coupling

Takahashi, et al. : Spin hydrodynamic generation, *Nature Physics* 12, 52–56 (2016)

1. Hg flowing down a channel
 - viscous forces with walls \Rightarrow fluid vorticity
2. Mechanical fluid vorticity $\Rightarrow e^-$ polarization
3. Gradient across channel \Rightarrow spin voltage
4. ... can be transformed into electrical voltage,
generators, etc. *without magnets*

"This opens a door to the new field of fluid spintronics"

(also an existence proof of $\vec{\omega} \leftrightarrow \vec{P}$ connection)



Local vorticity and polarization

- Fine-scale vorticity at the “point” cell is reflected in the *spin* of emitted particles

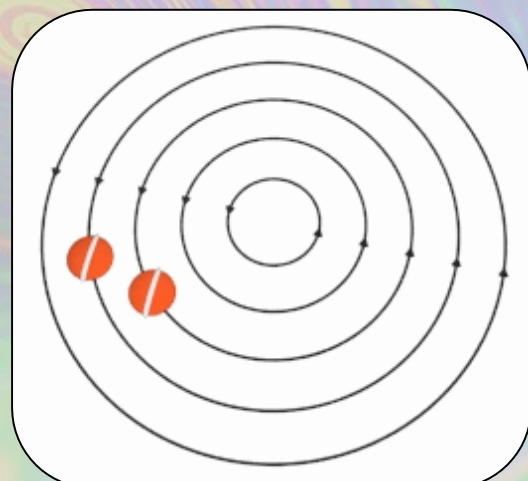
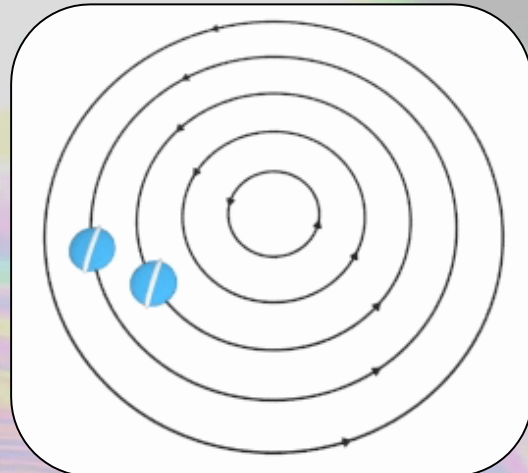
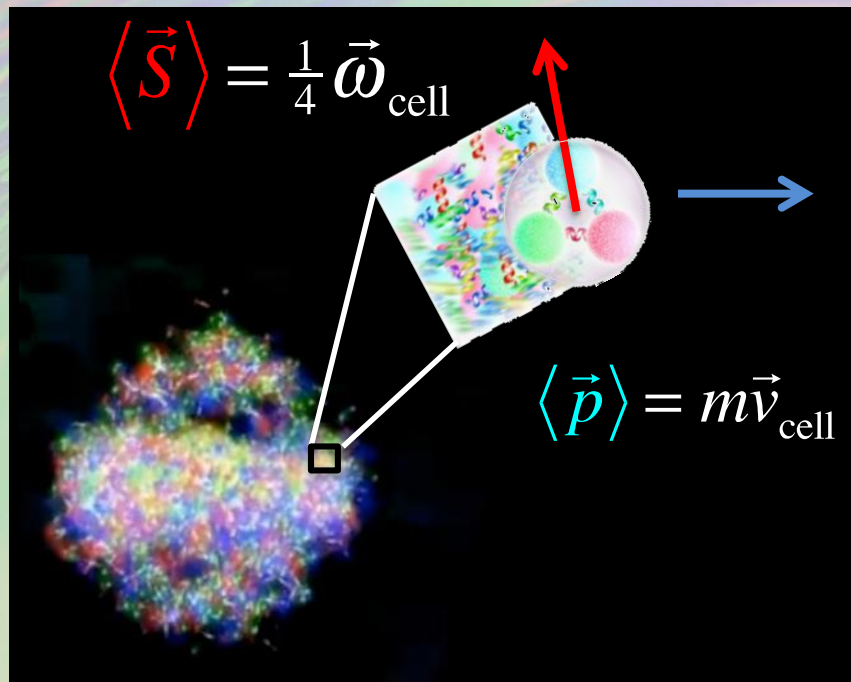
Polarization

$$\vec{P} \equiv \frac{\langle \vec{S} \rangle}{|\vec{S}|}$$

first suggested by

Betz *et al.*, Phys. Rev. C76
(2007) 044901

Becattini *et al.*, Phys. Rev. C77
(2008) 024906



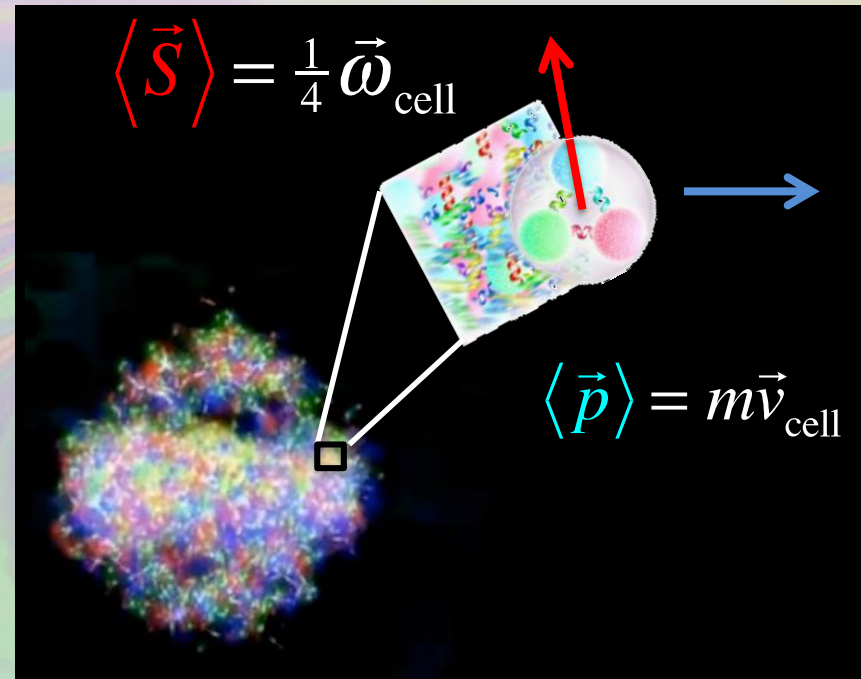
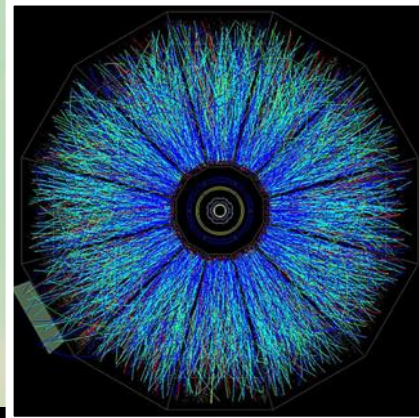
Subatomic spintronics

Barnett, Einstein-de Haas, Takahashi $\vec{P} \propto \vec{\omega}$
straightforward to measure both

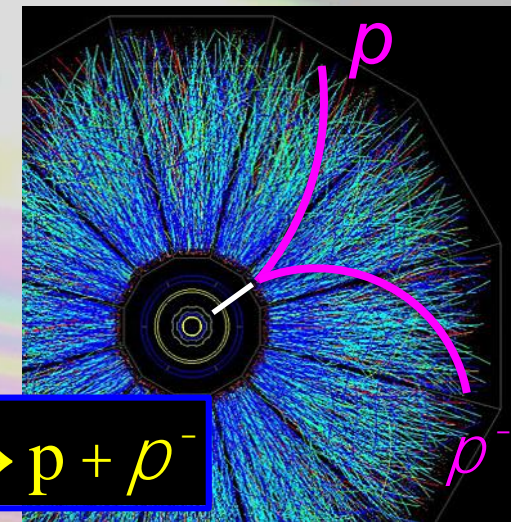
Our experimental situation is a little tougher...

1. how to measure polarization?
2. what is the *direction* of the vorticity?

...but we benefit from their validation of the connection



They had the electron, we have Λ



They had the electron, we have Λ

Lambdas are “self-analyzing”

- reveal polarization by preferentially emitting daughter proton in spin direction of Λ

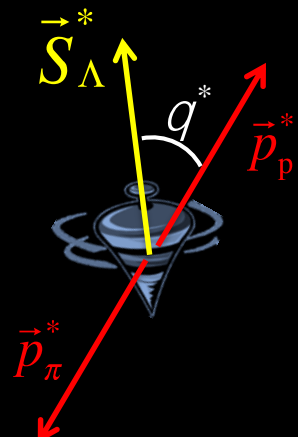
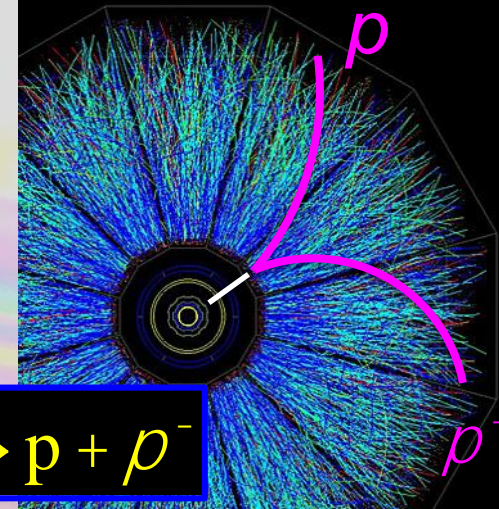
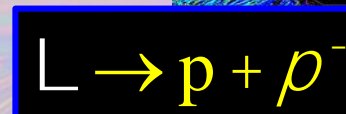
For an ensemble of Λ s with polarization \vec{P} :

$$\frac{dW}{d\Omega^*} = \frac{1}{4\pi} (1 + \alpha \vec{P} \cdot \hat{\vec{p}}_p^*) = \frac{1}{4\pi} (1 + \alpha P \cos \theta^*)$$

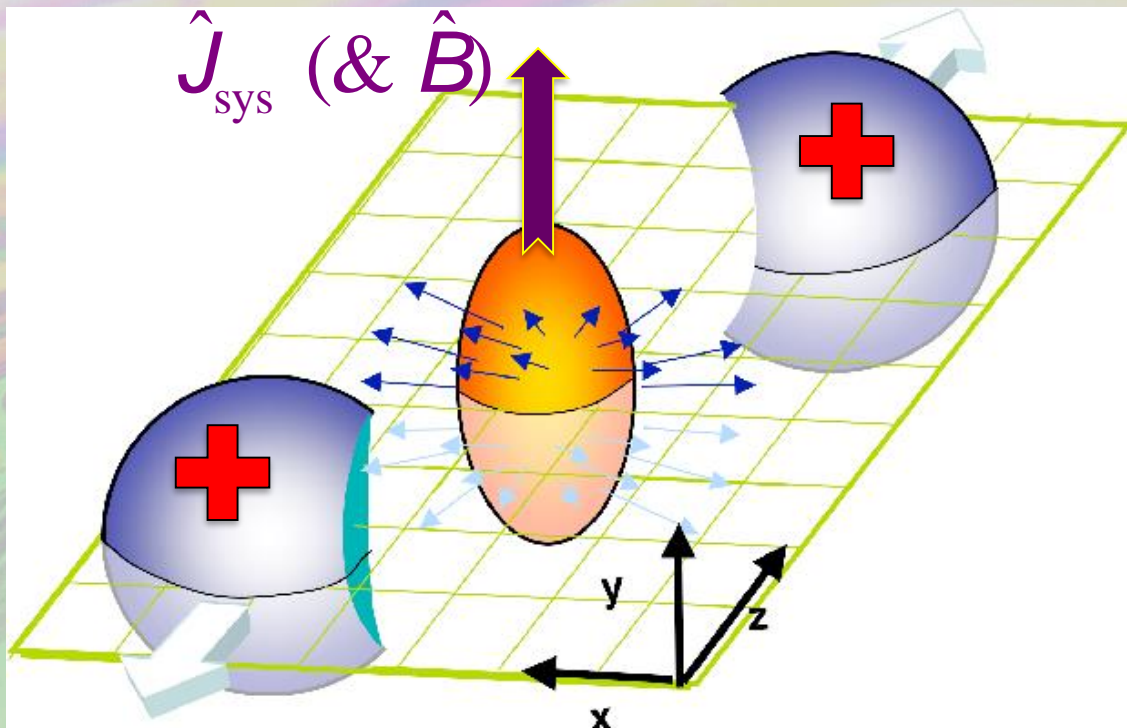
$\alpha = 0.642$ [measured]

$\hat{\vec{p}}_p^*$ is daughter proton momentum direction *in Λ frame*

$$0 < |\vec{P}| < 1: \quad \vec{P} = \frac{3}{\alpha} \hat{\vec{p}}_p^*$$



Global polarization – alignment of \vec{P} with $\hat{\mathbf{J}}_{\text{sys}}$



- LS coupling can generate a spin alignment, or polarization, along the direction of the vorticity in the local fluid cell, which, when averaged over the entire system, is parallel to \mathbf{J}_{sys} .

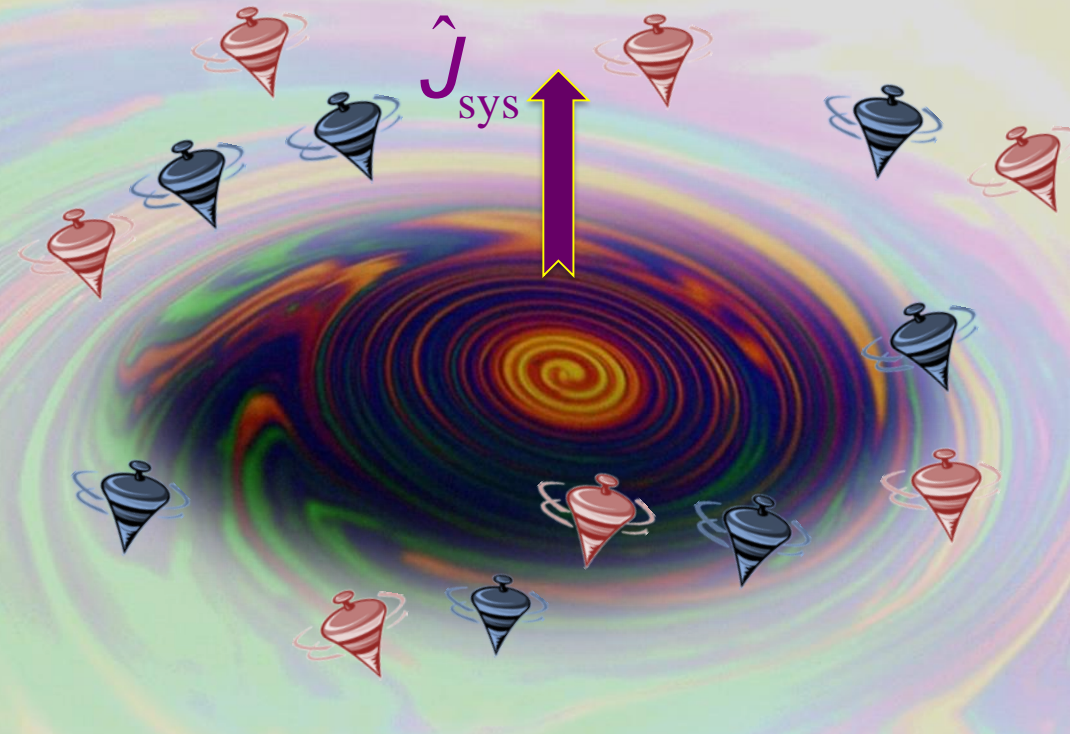
⇒ Polarization measurements of hadrons emitted from the fluid can be used to determine $\omega \equiv |\boldsymbol{\omega}|$.



Global polarization

Vortical coupling: $P \propto \omega$

$$\vec{P}_\Lambda \parallel +\hat{J}_{\text{sys}} \quad \vec{P}_{\bar{\Lambda}} \parallel +\hat{J}_{\text{sys}}$$





L



[

Global polarization

Vortical coupling: $P \propto \omega$

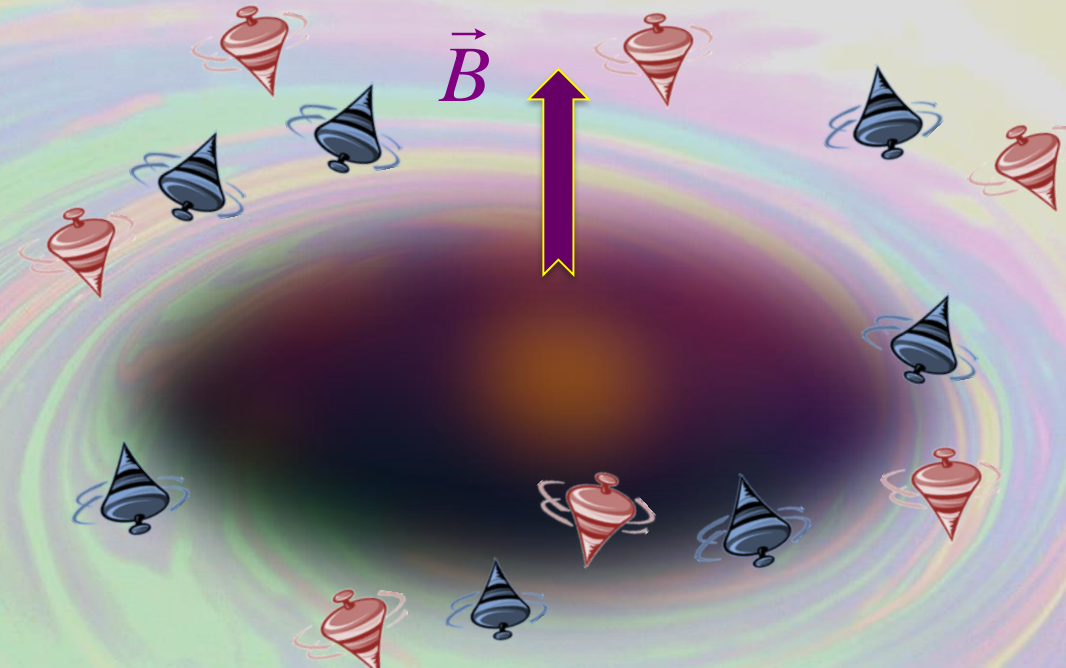
$$\vec{P}_\Lambda \parallel +\hat{J}_{\text{sys}} \quad \vec{P}_{\bar{\Lambda}} \parallel +\hat{J}_{\text{sys}}$$

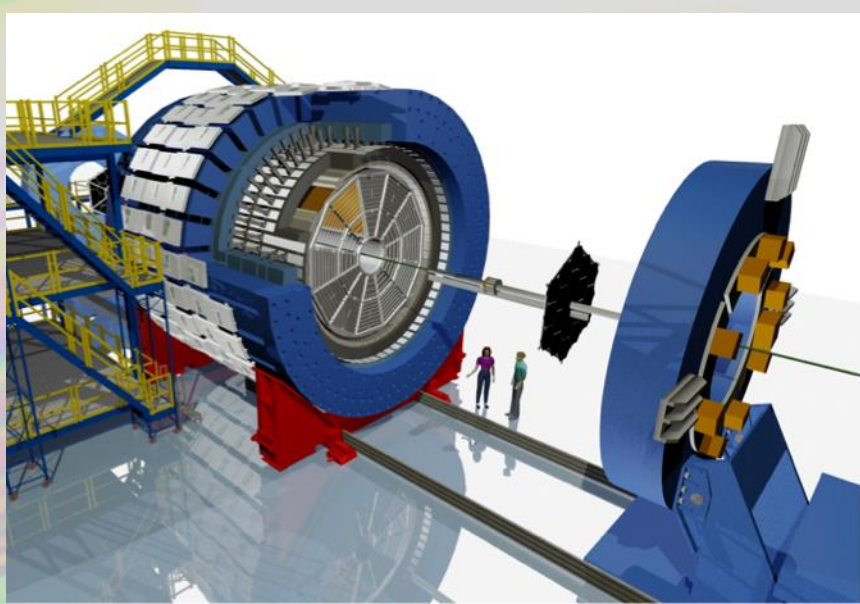
Magnetic coupling: $P \propto \vec{\mu} \cdot \vec{B}$

$$\vec{P}_\Lambda \parallel -\hat{J}_{\text{sys}} \quad \vec{P}_{\bar{\Lambda}} \parallel +\hat{J}_{\text{sys}}$$

N.B. $\mu_\Lambda = -0.613 \pm 0.04 \mu_N$

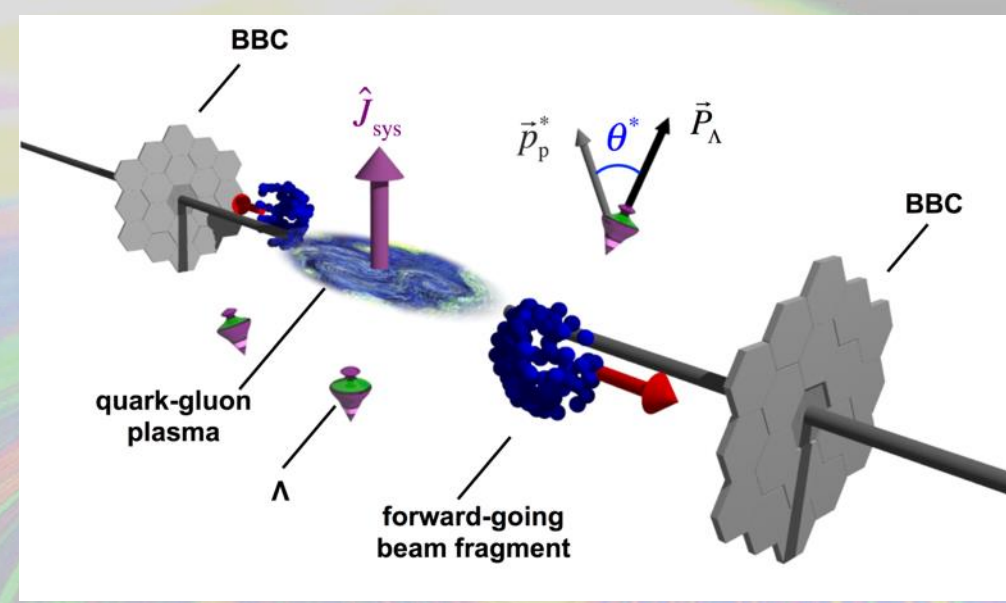
Both effects may be active



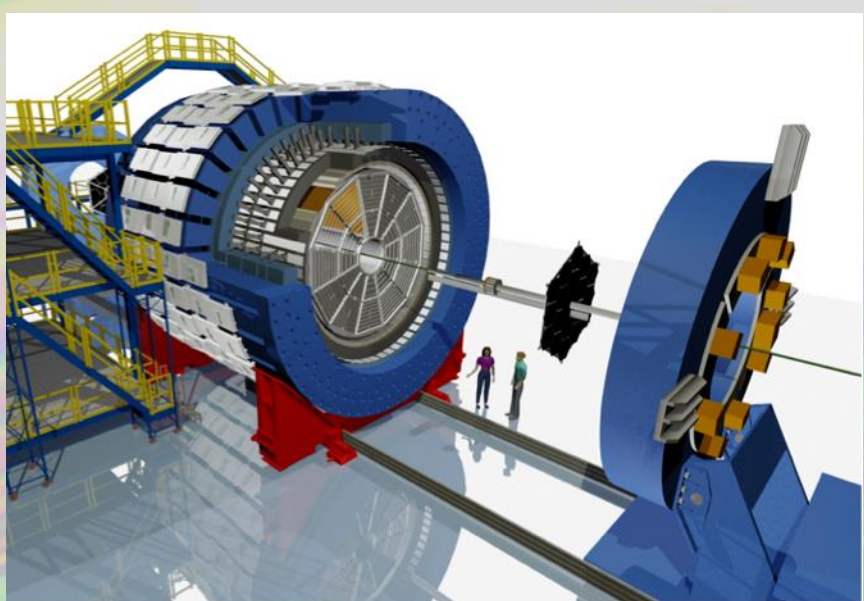


Λ , $\bar{\Lambda}$ reconstructed in TPC+TOF for $|y| < 1$

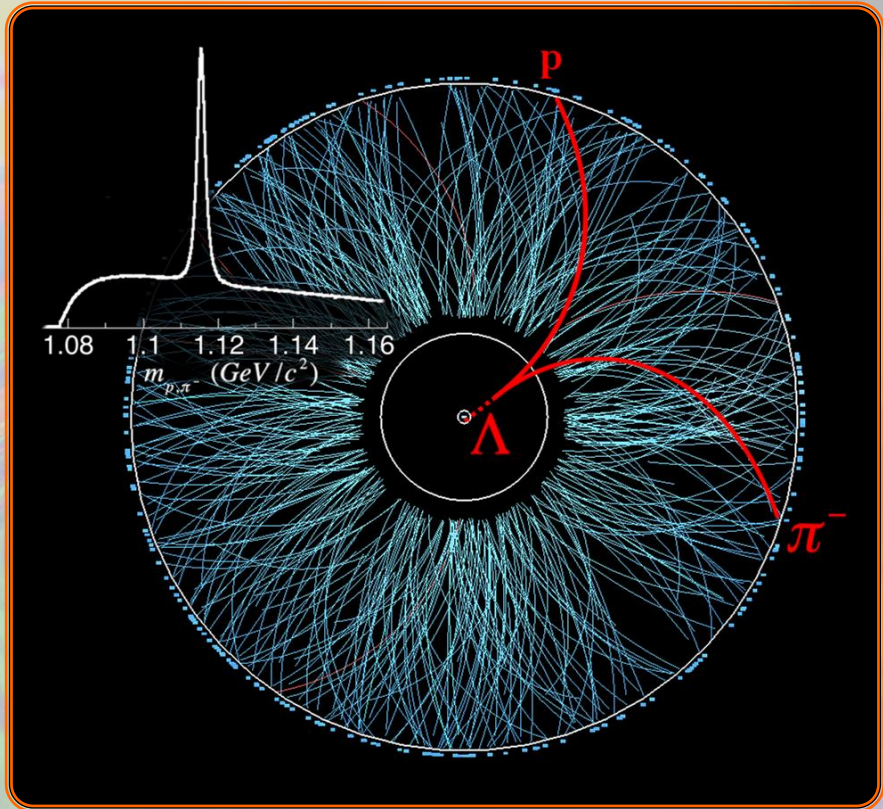
Our job: correlate \vec{p}_p^* and \hat{J}_{sys}



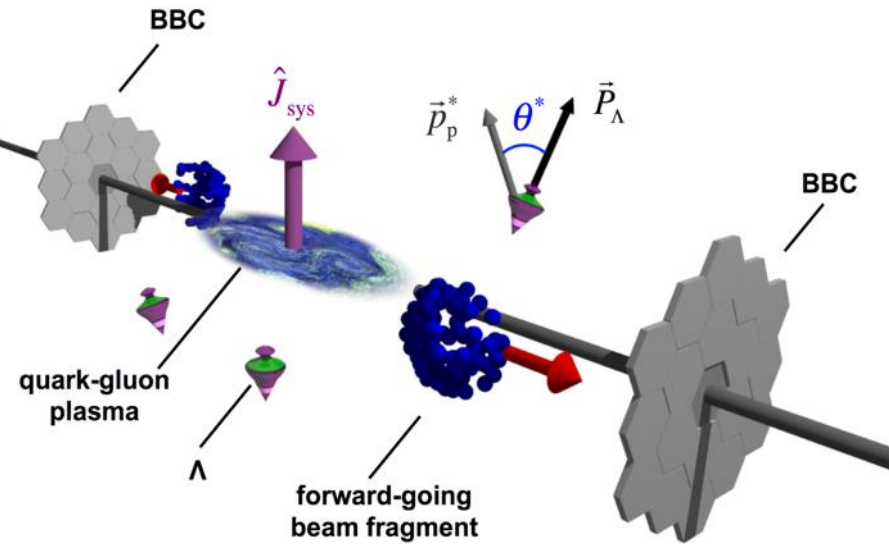
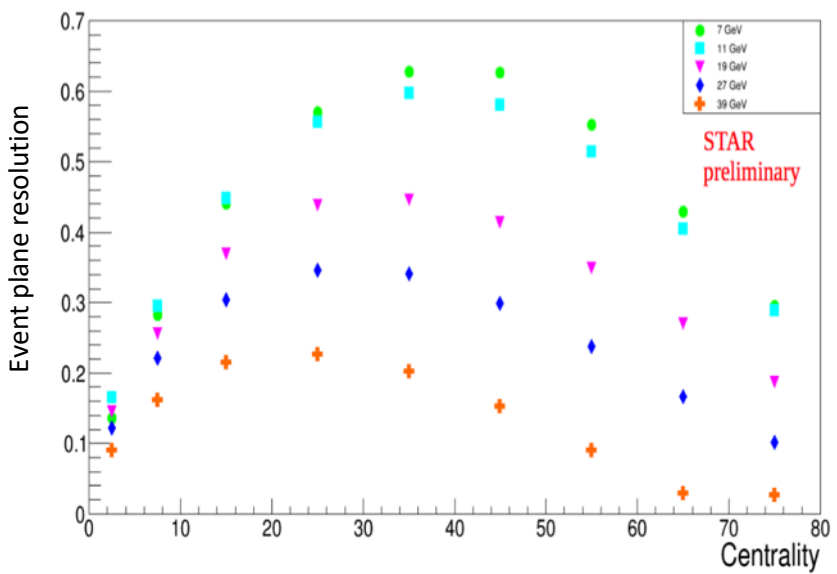
Forward BBCs estimate Reaction Plane: $\vec{B} \parallel \vec{\omega} \parallel \hat{J}_{\text{sys}}$



Λ , $\bar{\Lambda}$ reconstructed in TPC+TOF for $|y| < 1$



Lambdas are found topologically using identified protons and pions



Statistics-limited: average polarization, $\bar{P}_H \equiv \int d\vec{\beta}_\Lambda \frac{dN}{d\vec{\beta}_\Lambda} \vec{P}(\vec{\beta}_\Lambda) \cdot \hat{J}_{sys}$

$$\bar{P}_H = \frac{8}{\pi\alpha} \frac{\langle \sin(\phi_p^* - \Psi_{EP}^{(1)}) \rangle}{R_{EP}^{(1)}} \quad \text{where average is over events \& } \Lambda \text{s}$$

$\Psi_{EP}^{(1)}$ is the first-order event plane (from BBCs)

$R_{EP}^{(1)}$ is the first-order event plane resolution

Event-plane resolution $R_{EP}^{(1)}$

- obtained from correlation of two event plane vectors of two random sub-events
- best for mid-central collisions
- significantly worse at higher energy
- errorbars $d\bar{P}_H \propto \left(R_{EP}^{(1)} \sqrt{\# L} \right)^{-1}$

First global polarization signal

- Systematic uncertainty (dominated by combinatorial background) small relative to statistical uncertainty

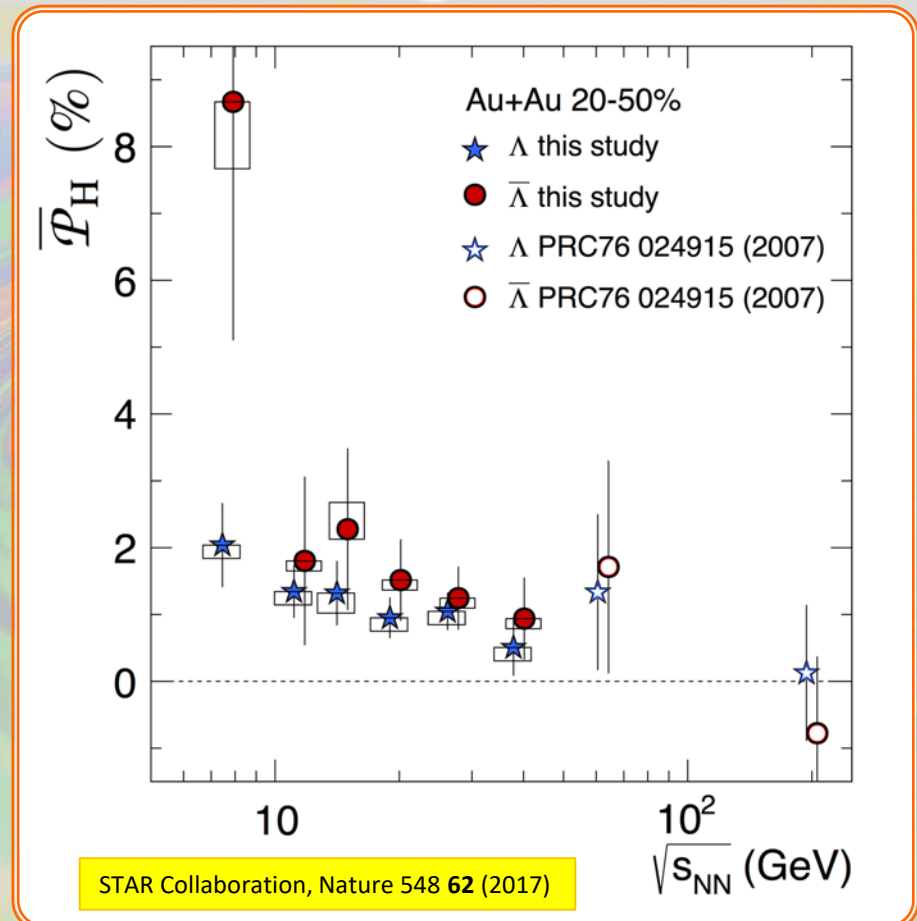
- vortical coupling dominant

$$\bar{P}_\perp \gg \bar{P}_{\bar{\perp}} > 0$$

- tantalizing suggestion (but no claim!) of additional magnetic coupling

$$\bar{P}_{\bar{\perp}} > \bar{P}_\perp \quad ???$$

- Signal falls with energy (large errorbars...)
 - previous “null” result in line with the trend



First global polarization signal

- Systematic uncertainty (dominated by combinatorial background) small relative to statistical uncertainty

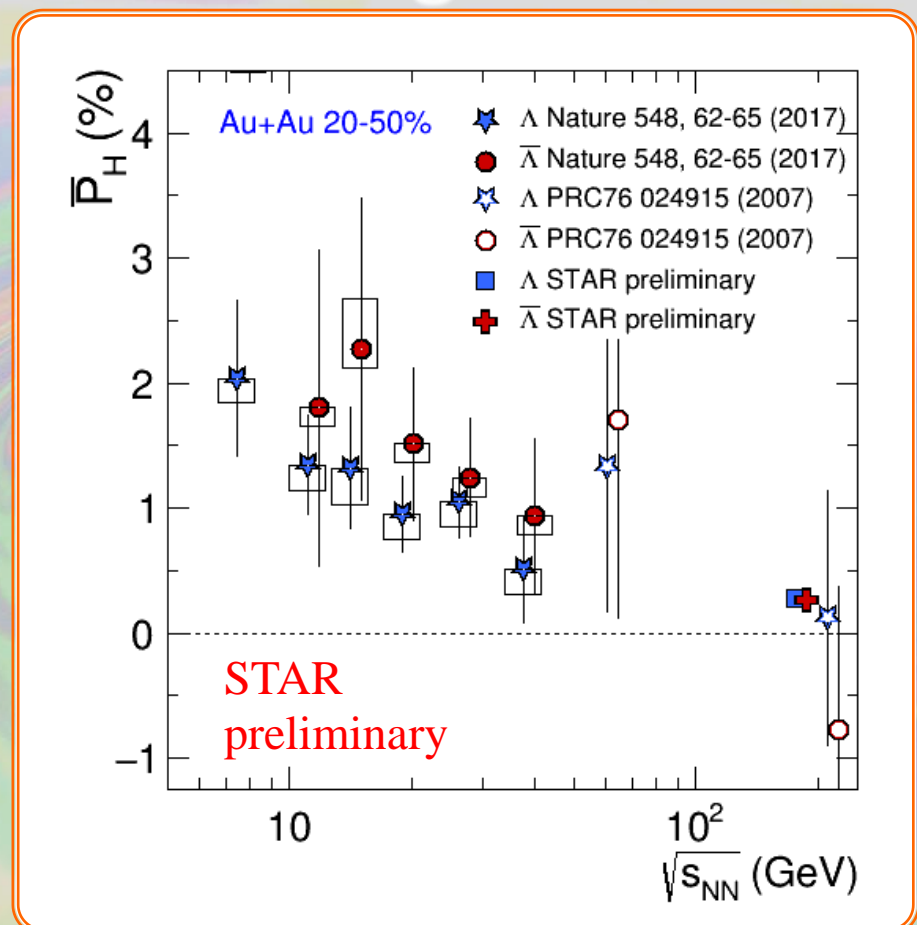
- vortical coupling dominant

$$\bar{P}_\perp \gg \bar{P}_\parallel > 0$$

- tantalizing suggestion (but no claim!) of additional magnetic coupling

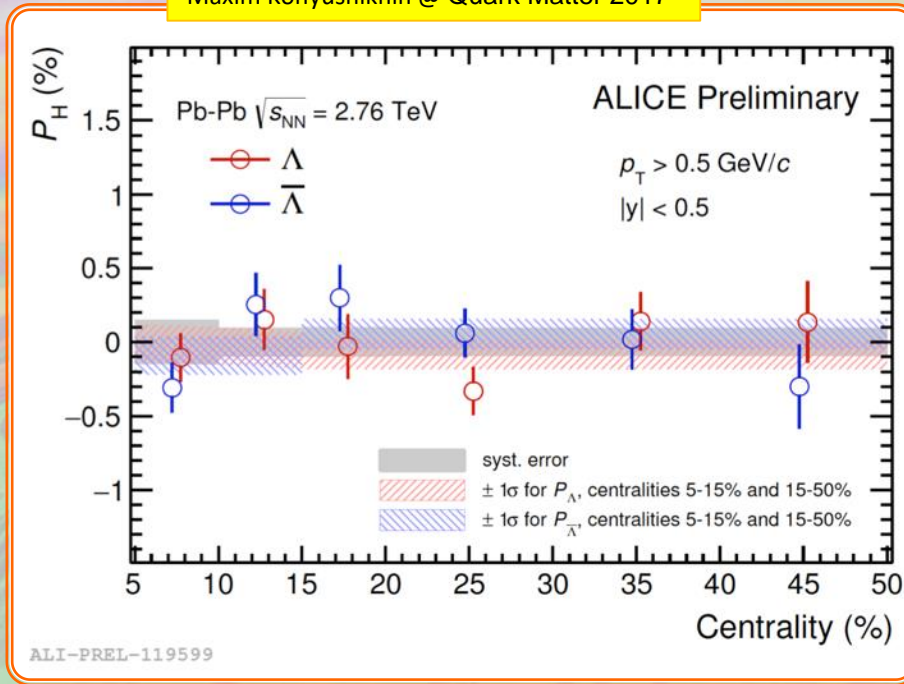
$$\bar{P}_\parallel > \bar{P}_\perp \quad ???$$

- Signal falls with energy (large errorbars...)
 - previous “null” result in line with the trend



Results from LHC (ALICE)

Maxim Konyushikhin @ Quark Matter 2017



$$\begin{aligned} \text{5-15% centrality} &= \begin{cases} P_\Lambda = -0.0001 \pm 0.0013(\text{stat}) \pm 0.0004(\text{syst}) \\ P_{\bar{\Lambda}} = -0.0009 \pm 0.0013(\text{stat}) \pm 0.0008(\text{syst}) \end{cases} \\ \text{15-50% centrality} &= \begin{cases} P_\Lambda = -0.0008 \pm 0.0010(\text{stat}) \pm 0.0004(\text{syst}) \\ P_{\bar{\Lambda}} = 0.0005 \pm 0.0010(\text{stat}) \pm 0.0003(\text{syst}) \end{cases} \end{aligned}$$

Pb-Pb@2.76 TeV:

All available ALICE [Pb-Pb@2.76](#) TeV data was analyzed.

The measured polarizations of Λ and $\bar{\Lambda}$ hyperons are compatible with expectations and are consistent with zero within the precision of the measurement.

Expected significance of the combined $\Lambda + \bar{\Lambda}$ result is at 1σ level.

3σ significance requires 10 x more data.

Pb-Pb@5.02 TeV:

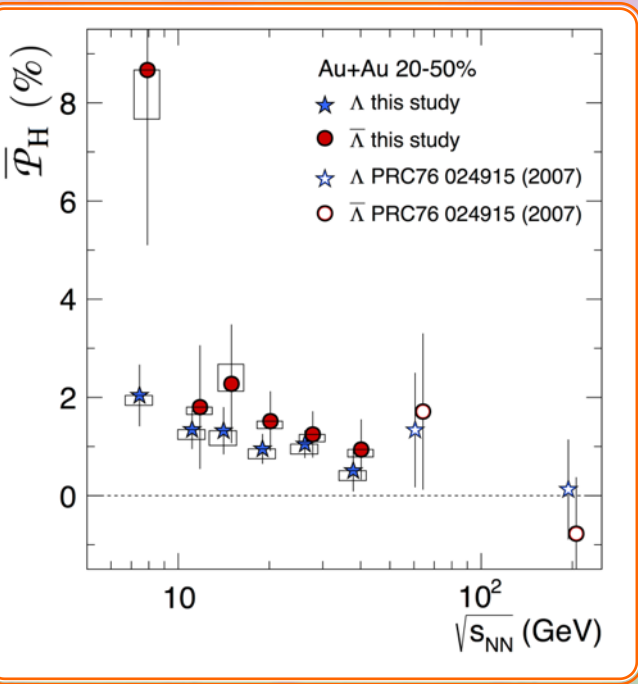
Assuming same ZDC event plane resolution and same feed-down:

Polarization is expected to decrease very slowly with collision energy.

The measurement becomes more feasible at higher collision energies due to a faster increase of the hyperon yield*.

*up to $\sim \sqrt{2}$ better significance due to $\times 2$ more hyperons with similar amount of events.

Extracting vorticity and magnetic field



Magneto-hydro equilibrium interpretation

$$\text{Prob} \sim \exp\left(-E/T + \mu_B B/T + \vec{\omega} \cdot \vec{S}/T + \vec{\mu} \cdot \vec{B}/T\right)$$

for small polarization: $P_L \gg \frac{1}{2} \frac{W}{T} - \frac{m_L B}{T}$ $P_{\bar{L}} \gg \frac{1}{2} \frac{W}{T} + \frac{m_{\bar{L}} B}{T}$

vorticity from sum: $\frac{W}{T} = P_L + P_{\bar{L}}$

B-field from difference: $\frac{B}{T} = \frac{1}{2m_L} (P_{\bar{L}} - P_L)$

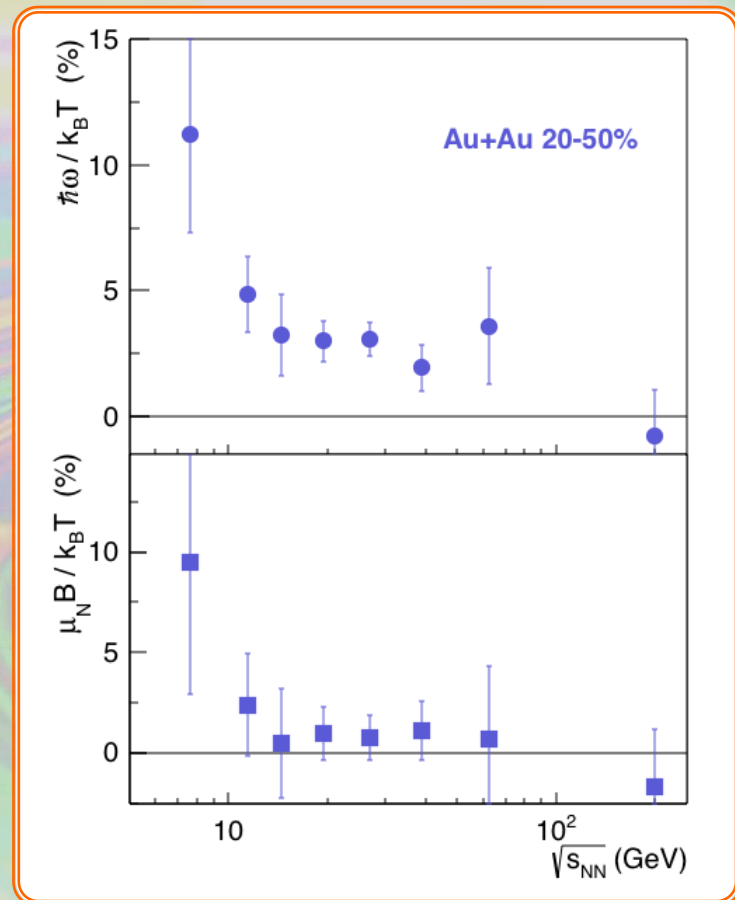
Extracted Physical Parameters

Significant vorticity signal

- $P_{\text{primary}} = \frac{W}{2T} \gg 5\%$
- (probably) falling with collision energy, despite increasing J_{sys}

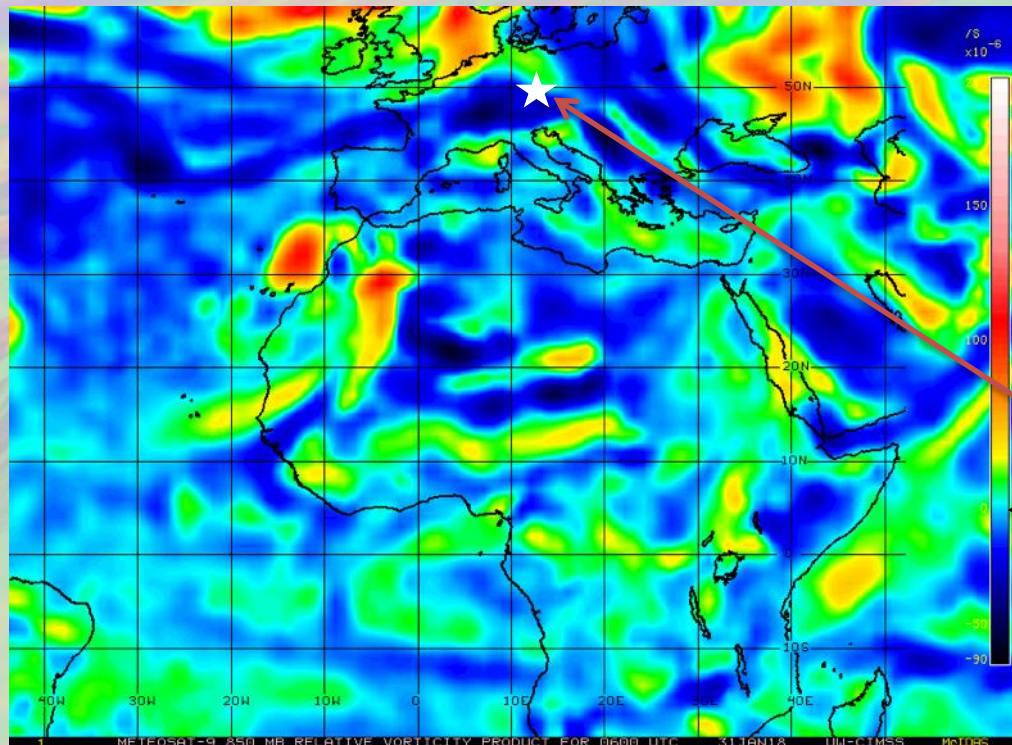
Magnetic field

- positive value would be expected
- 2σ above zero, *averaged* over all BES energies
- Higher statistics dataset for 27 GeV in run 2018 \Rightarrow hope for 5σ measurement

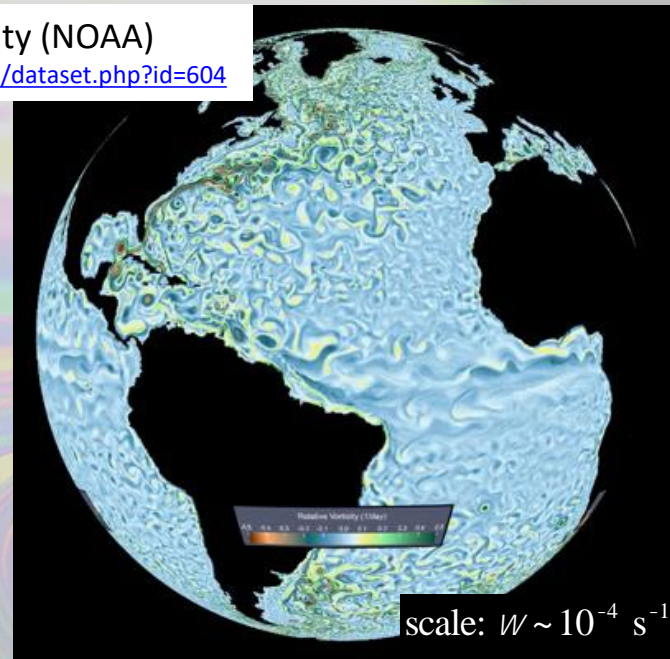


Perspective

- ocean flows: $\omega \sim 10^{-5} \text{ s}^{-1}$
- terrestrial atmosphere: $\omega \sim 10^{-4} \text{ s}^{-1}$



Ocean surface vorticity (NOAA)
<http://sos.noaa.gov/Datasets/dataset.php?id=604>



Praha

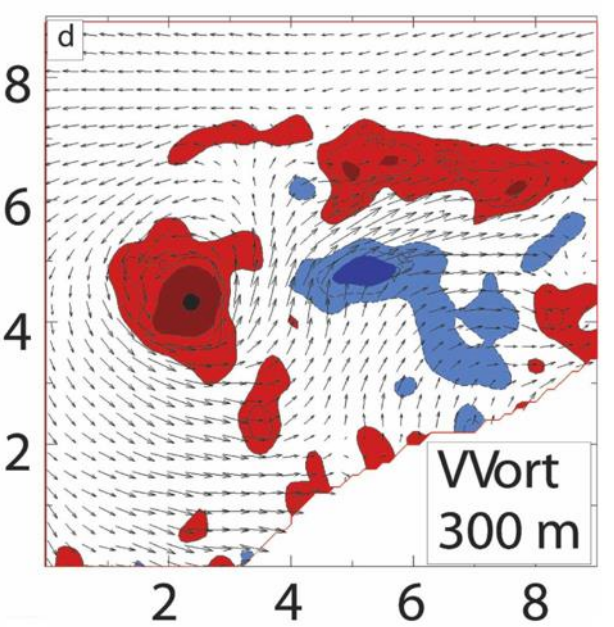
zero

vorticity as of 10:00 31 Jan 2018

<http://tropic.ssec.wisc.edu/real-time/europe/winds/wm1vor.GIF>

Perspective

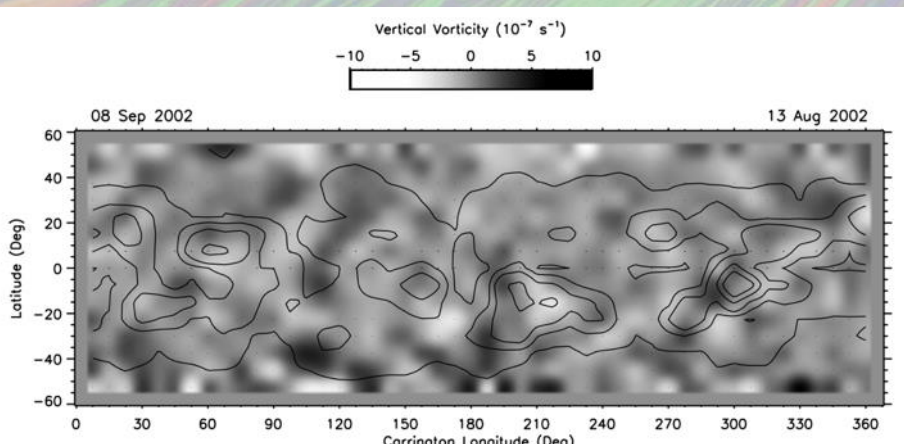
- ocean flows: $\omega \sim 10^{-5} \text{ s}^{-1}$
- terrestrial atmosphere: $\omega \sim 10^{-4} \text{ s}^{-1}$
- core of supercell tornado: $\omega \sim 10^{-1} \text{ s}^{-1}$



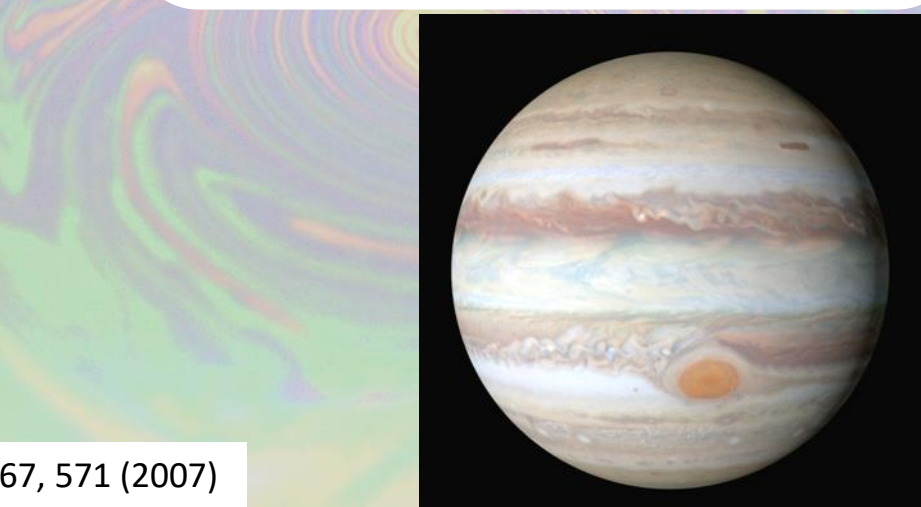
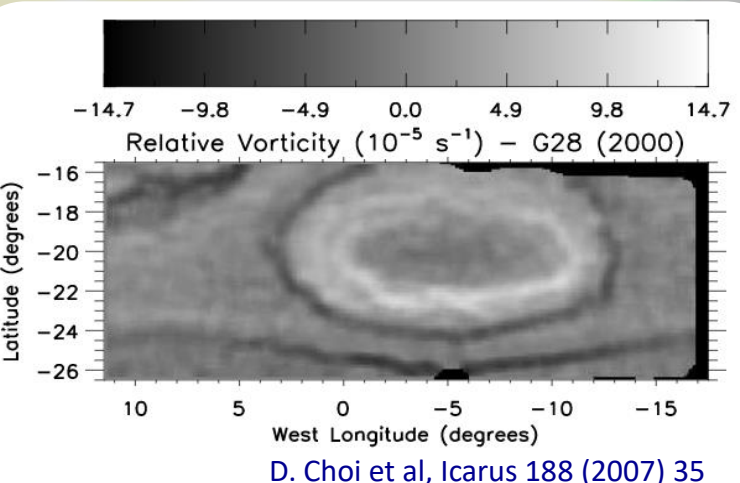
Doppler radar measurement of supercell tornado system tornado,
21 May 1998, Bridgeport, Nebraska
J. Wurman *et al.*, Mon. Weather Rev. 135, 2392 (2007)

Perspective

- ocean flows: $\omega \sim 10^{-5} \text{ s}^{-1}$
- terrestrial atmosphere: $\omega \sim 10^{-4} \text{ s}^{-1}$
- core of supercell tornado: $\omega \sim 10^{-1} \text{ s}^{-1}$
- solar subsurface flow: $\omega \sim 10^{-6} \text{ s}^{-1}$
- “Collar” of Jupiter’s Great Red Spot: $\omega \sim 10^{-4} \text{ s}^{-1}$

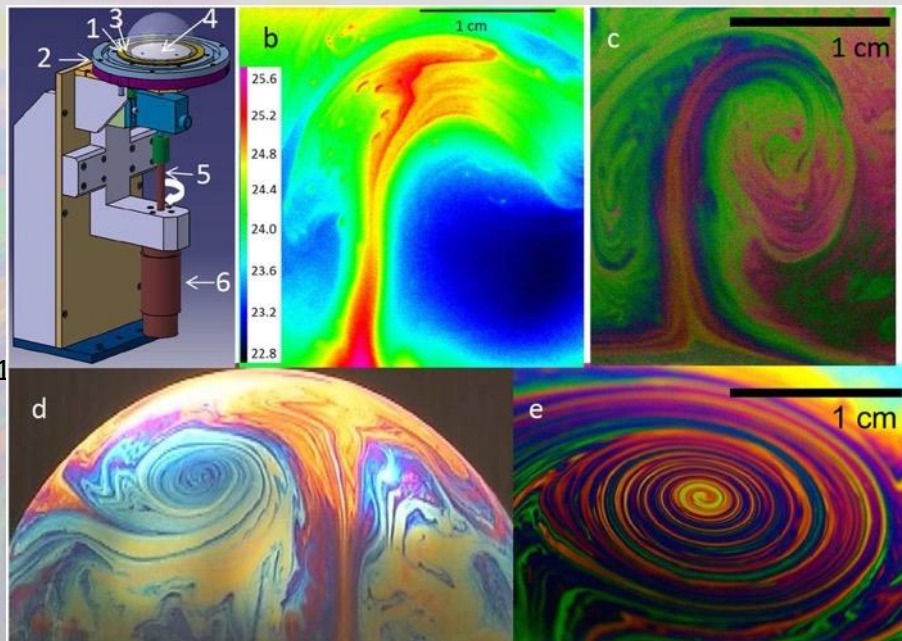


solar subsurface vorticity, 2002 R. Komm *et al.*, *Astrophys. J.* 667, 571 (2007)



Perspective

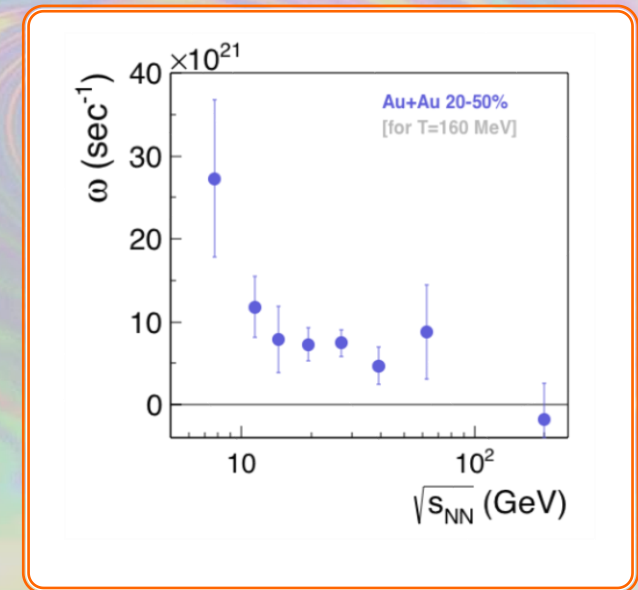
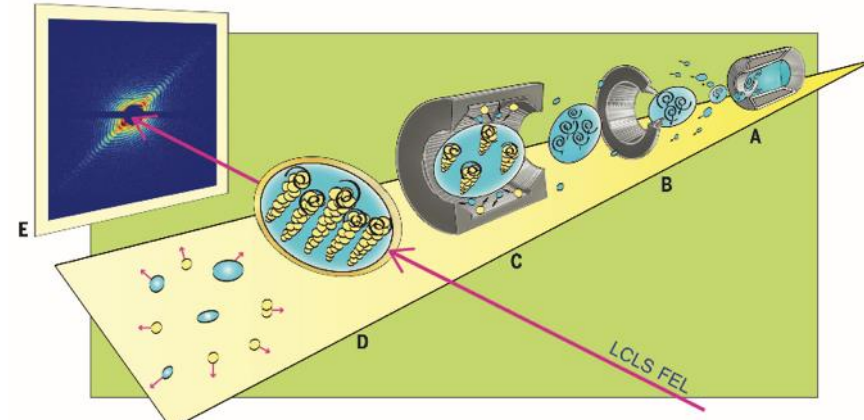
- ocean flows: $\omega \sim 10^{-5} \text{ s}^{-1}$
- terrestrial atmosphere: $\omega \sim 10^{-4} \text{ s}^{-1}$
- core of supercell tornado: $\omega \sim 10^{-1} \text{ s}^{-1}$
- solar subsurface flow: $\omega \sim 10^{-6} \text{ s}^{-1}$
- “Collar” of Jupiter’s Great Red Spot: $\omega \sim 10^{-4} \text{ s}^{-1}$
- Heated, rotating soap bubbles: $\omega \sim 10^2 \text{ s}^{-1}$



Intensity of vortices: from soap bubbles to hurricanes
T. Meuel, et al, (Nature) Scientific Reports **3** 3455 (2013)

World's record

- ocean flows: $\omega \sim 10^{-5} \text{ s}^{-1}$
- terrestrial atmosphere: $\omega \sim 10^{-4} \text{ s}^{-1}$
- core of supercell tornado: $\omega \sim 10^{-1} \text{ s}^{-1}$
- solar subsurface flow: $\omega \sim 10^{-6} \text{ s}^{-1}$
- “Collar” of Jupiter’s Great Red Spot: $\omega \sim 10^{-4} \text{ s}^{-1}$
- Heated, rotating soap bubbles: $\omega \sim 10^2 \text{ s}^{-1}$
- Max vorticity in bulk superfluid He-II: $\omega \sim 150 \text{ s}^{-1}$
R. Donnelly, Ann. Rev. Fluid Mech. 25, 325 (1993)
- Max vorticity in nanodroplets of superfluid He-II: 10^6 s^{-1}
Gomez et al, Science 345 (2014) 903



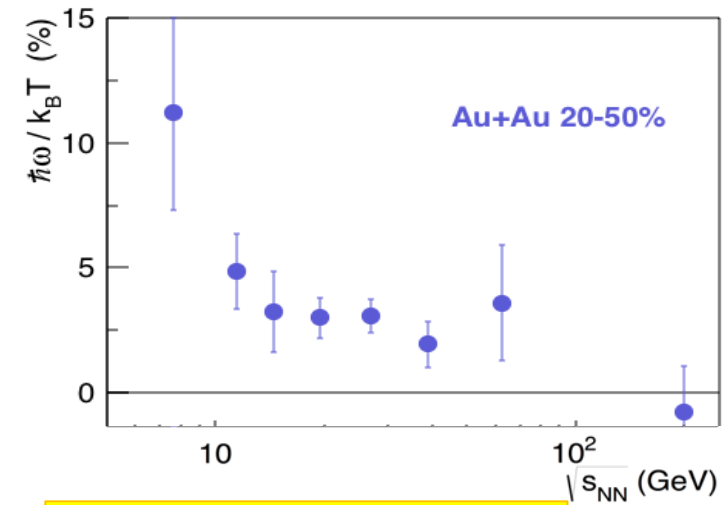
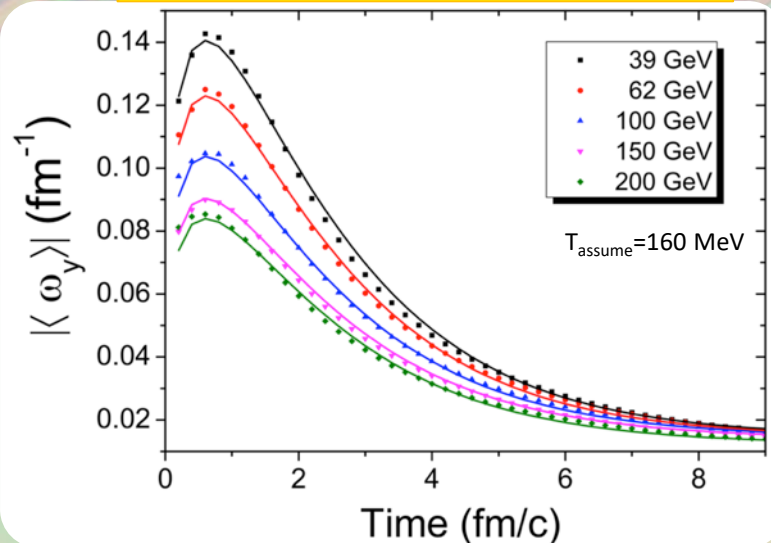
Vorticity \sim theory expectation

Thermal vorticity $\omega/T = 2-10\%$

$\rightarrow \omega = 0.02-0.09 \text{ fm}^{-1}$

\rightarrow Magnitude, vs-dep in range of transport & 3D viscous hydro calculations with rotation

Y. Jiang, Z.W. Lin and J. Liao, Phys. Rev.C 94, 044910 (2016)



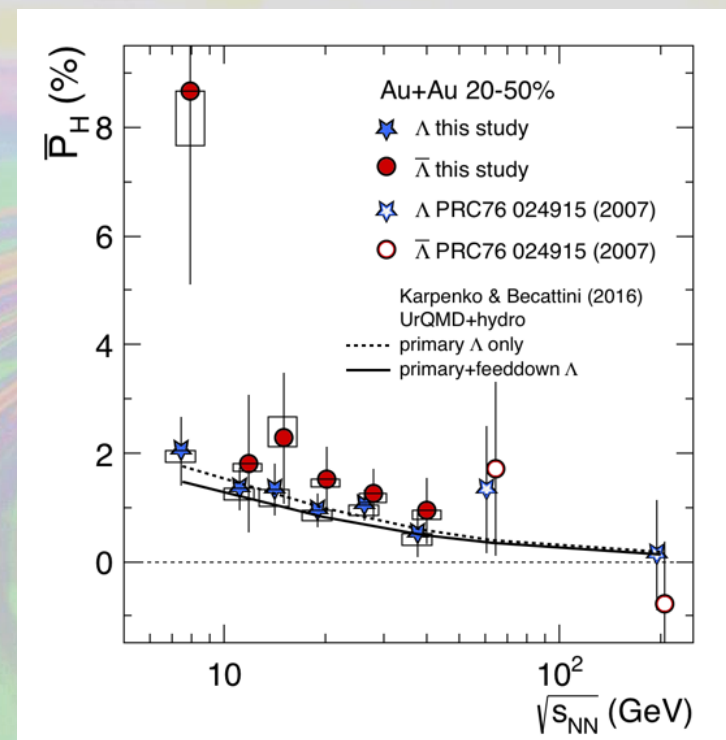
L. Csernai et al., Phys. Rev. C90, 021904(R) (2014)

TABLE I. Time dependence of average vorticity projected to the reaction plane for heavy-ion reactions at the NICA energy of $\sqrt{s_{NN}} = 4.65 + 4.65 \text{ GeV}$.

t (fm/c)	Vorticity (classical) (c/fm)	Thermal vorticity (relativistic) (1)
0.17	0.1345	0.0847
1.02	0.1238	0.0975
1.86	0.1079	0.0846
2.71	0.0924	0.0886
3.56	0.0773	0.0739

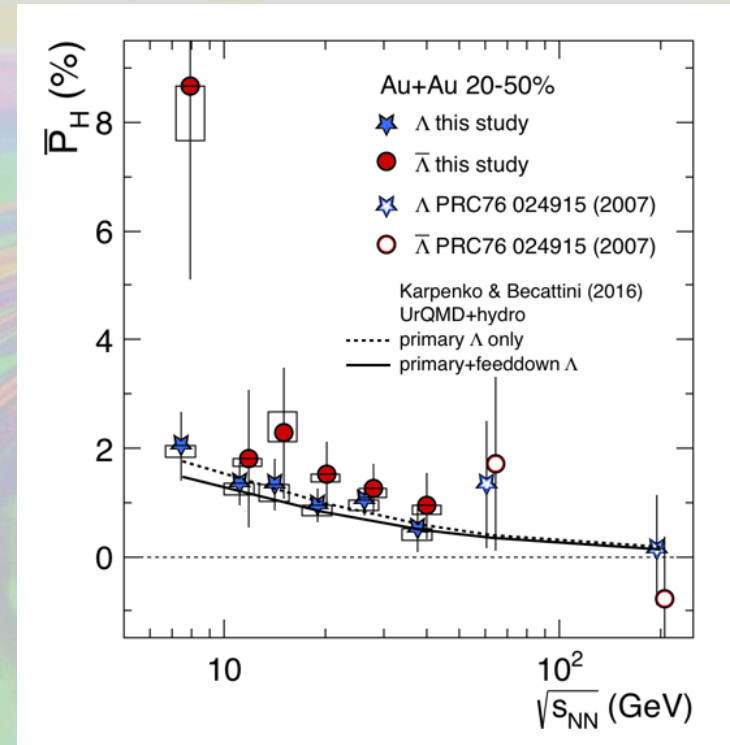
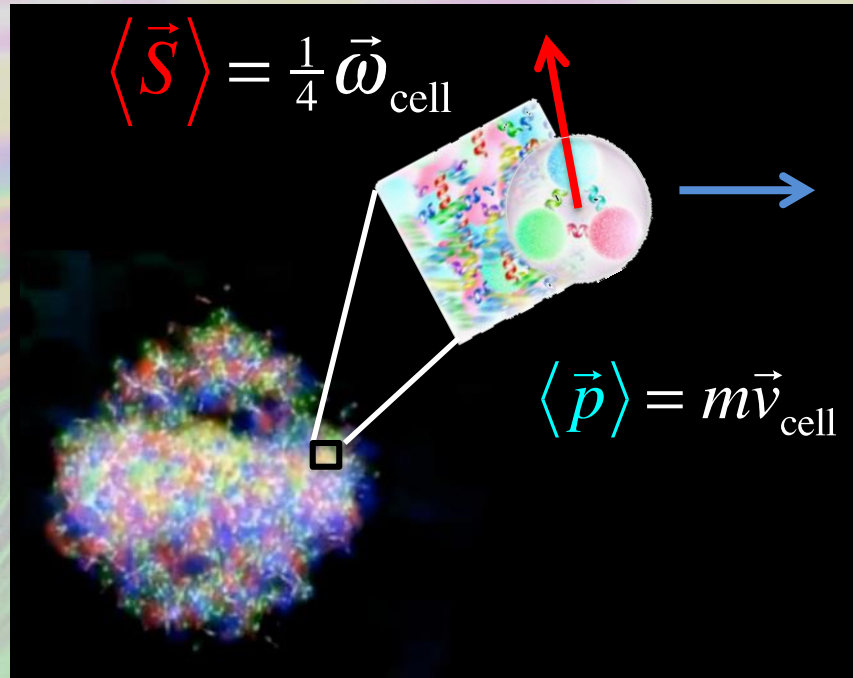
Direct comparison with 3D calculation

- UrQMD (lumpy conditions) + hydro
- matching & evolution parameters tuned to reproduce $dN/d\eta$, dN/dp_T , v_2 (*but not ω !*)
- strong dependence on lumpiness of initial conditions given by UrQMD



Theory: Becattini, Karpenko, EPJ C77(2017)213

A key take-away



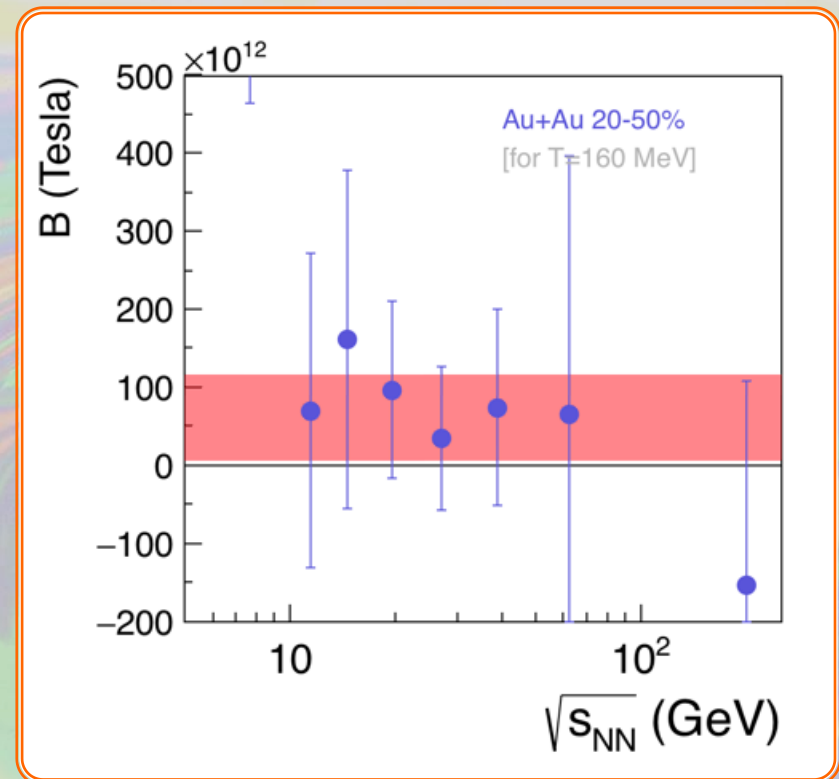
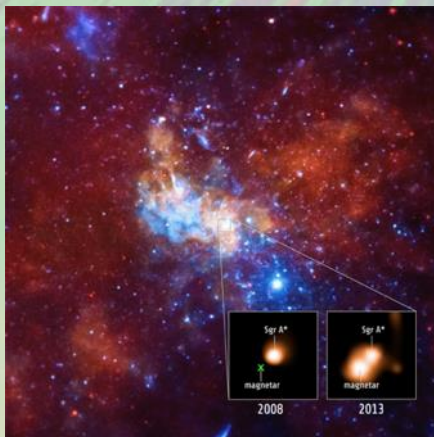
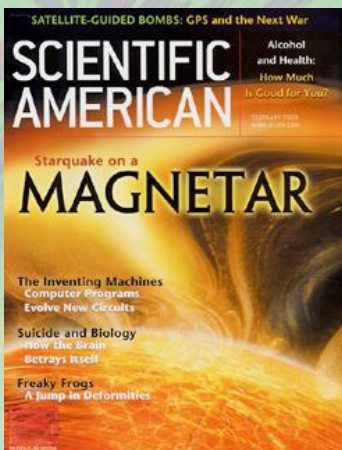
This is a stunning success and validation of the hydro paradigm underlying our understanding of heavy ion collisions. The substructure of the prediction is being tested at a much finer level than “just” anisotropy of the momentum distribution

Magnetic field?

- Statistical uncertainties preclude claim
- B should change with energy, but...

$$\langle B \rangle_{\sqrt{s}} = 6.0 \pm 5.5 \times 10^{13} \text{ T}$$

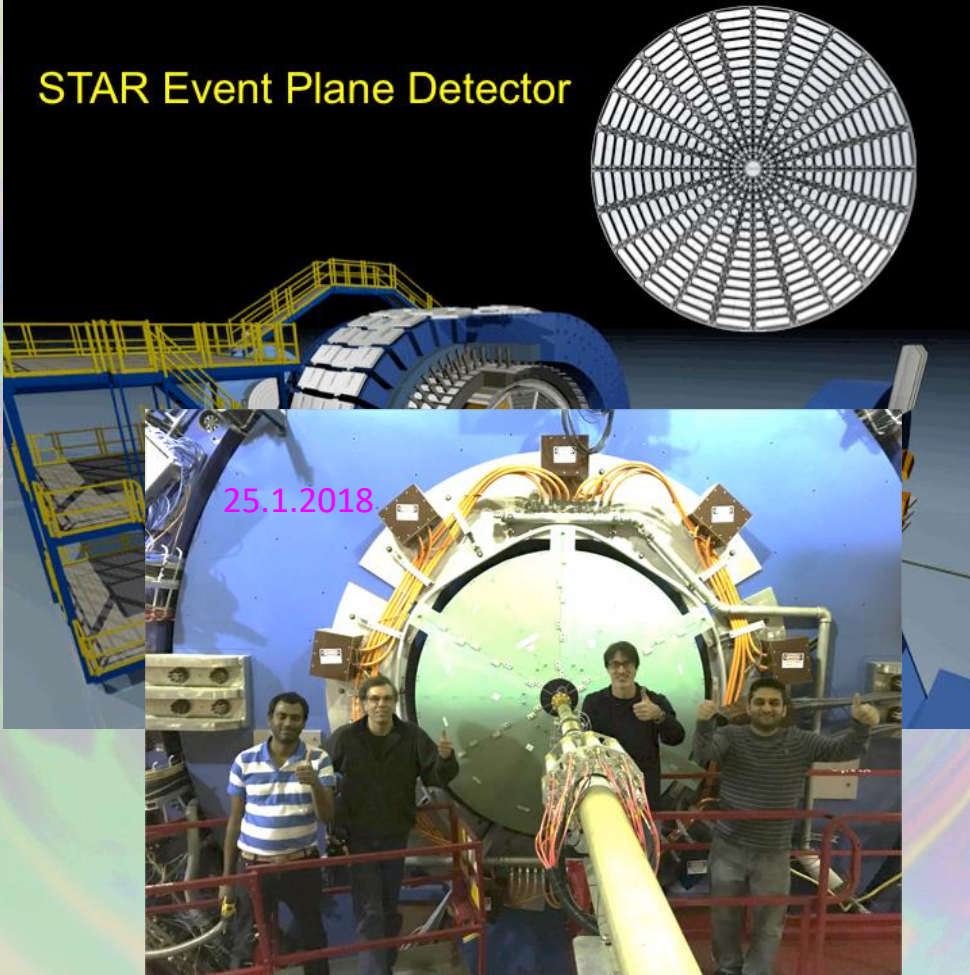
- Highest fields in the known universe:
Magnetars $\sim 10^{10}\text{-}10^{11}$ T



McGill Online Magnetar Catalog: ApJS 212 (2014)
<http://www.physics.mcgill.ca/~pulsar/magnetar/main.html>

Coming up

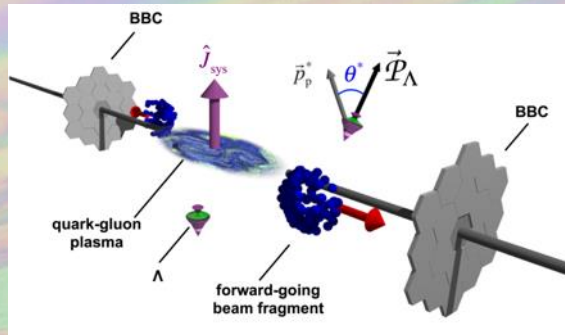
- ω & B : of very high interest to the field
 - model substructure
 - dedicated workshops
 - novel QCD effects (CME, CVE)
- Based on this discovery, BNL approved
2 weeks dedicated running in 2018
 - further exploration in 2019+
- STAR upgrade detector – EPD
 - project led & built by OSU (M. Lisa)
 - significant improvement on \hat{J} resolution



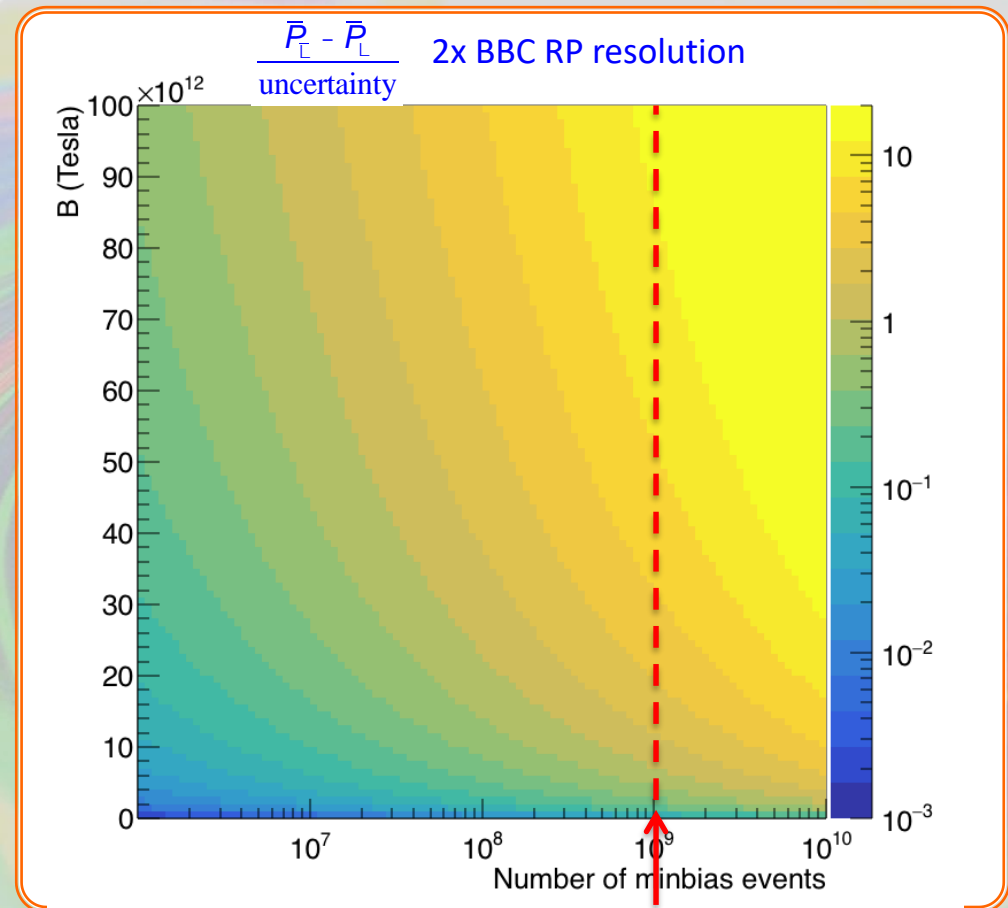
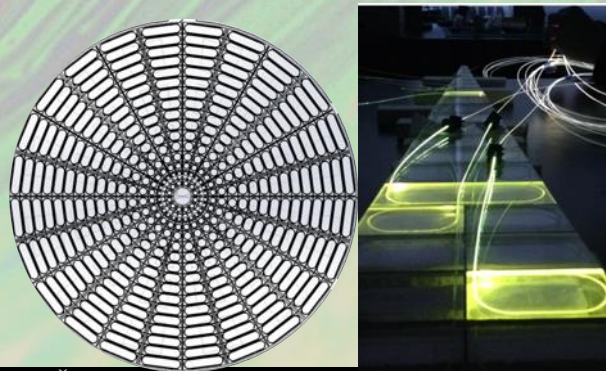
Magnetic splitting? 2018 run at 27 GeV

Expect fields $\sim 5 \times 10^{13}$ T (for how long?)

BES-I: 67×10^6 min. bias events with BBC

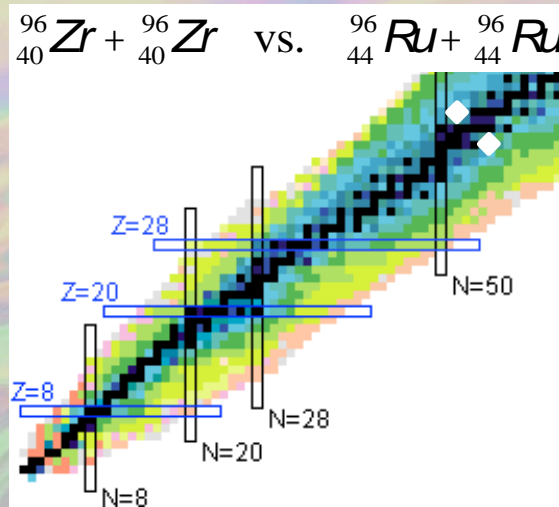


2018 : 10^9 events & detector upgrade

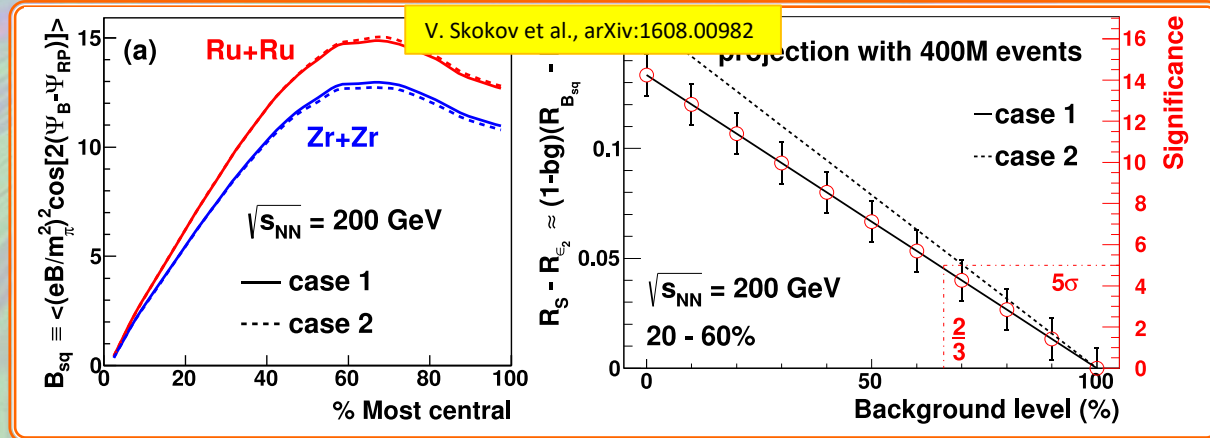


Chiral Magnetic Effect: 2018 run at 200 GeV

Expect fields $\sim 5 \times 10^{13}$ T (for how long?)



Zr and Ru same geometry and mass;
charge different by 10% (20% signal difference)
5 σ effect with 20% (signal)+80% (background)



Beam Energy (GeV/nucleon)	$\sqrt{s_{NN}}$ (GeV)	Run Time	Species	Number Events	Priority	Sequence
100	200	3.5 weeks	Ru+Ru	1.2B MB	1	1
100	200	3.5 weeks	Zr+Zr	1.2B MB	1	2
13.5	27	3 weeks	Au+Au	1B MB	2	4
3.85	3.0 (FXT)	2 days	Au+Au	100M MB	3	5

Blind analyses of CME studies of Run-18 isobar data:

- “Frequent” switching of isobar collision species
- **Interleave** isobar data samples from each species
- Respect the **time-variation** of running conditions

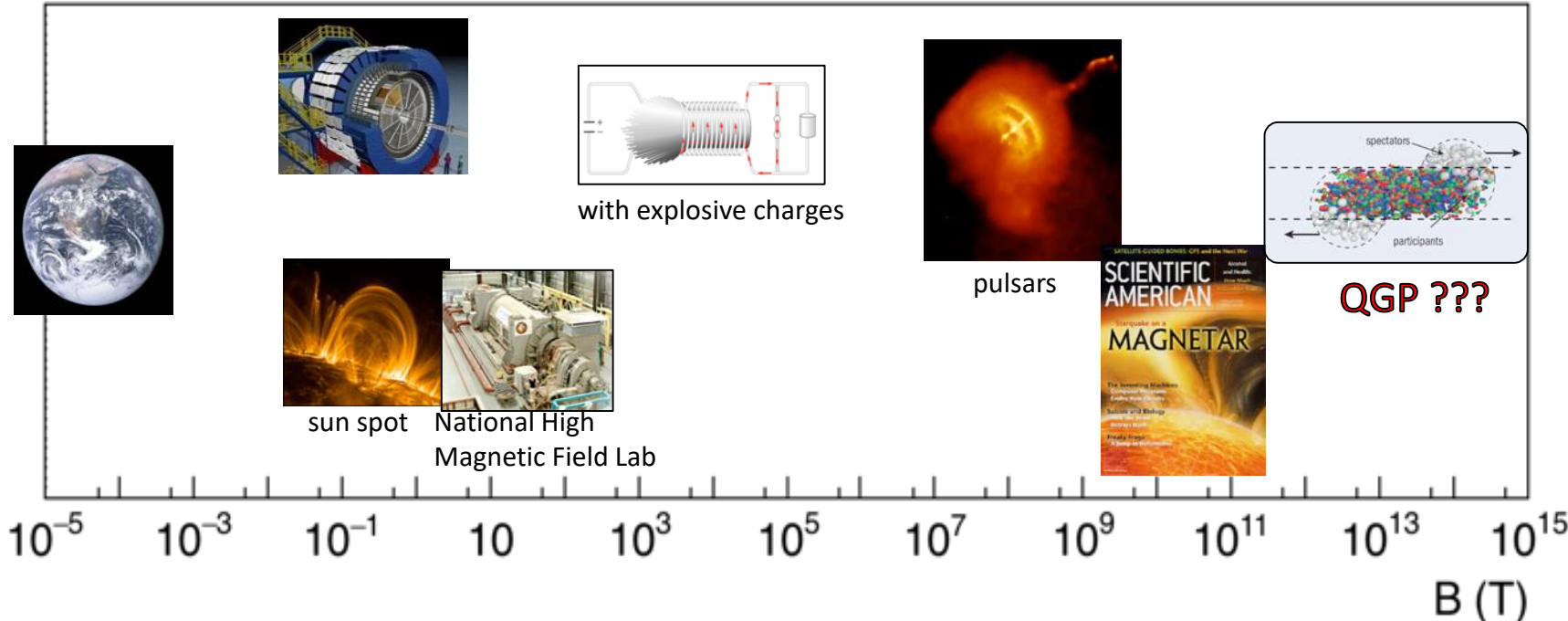
Summary

- First observation of global polarization by STAR@RHIC
- Interpretation in magnetic-vortical model:
 - clear vortical component of expected sign & magnitude for BES energies
 - magnetic component consistent with zero, but tantalizing hint that STAR pursues in 2018 & BES-II
- stunning success/validation of hydro picture
 - subjected to unique probe of substructure considerably finer than previously achieved
 - much more can be done to probe substructure of the substructure
- non-central H.I. collisions create most vortical fluid observed to date
 - generated by early shear viscosity, persists through low viscosity
- Vorticity & B-field crucial elements to validate/calibrate high-profile CME & CVE measurements @ RHIC

THANKS FOR YOUR ATTENTION



Intermezzo: Magnetic Fields in A+A

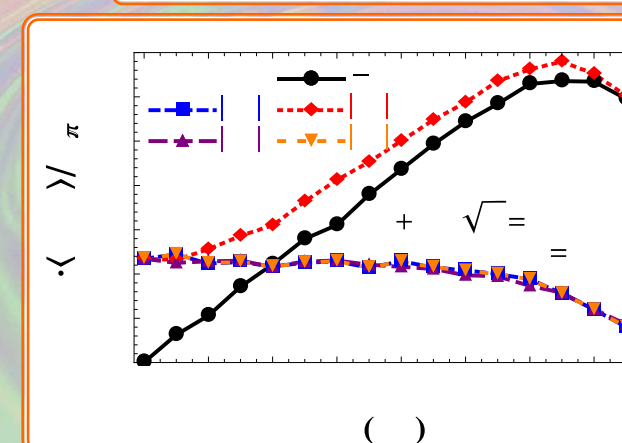
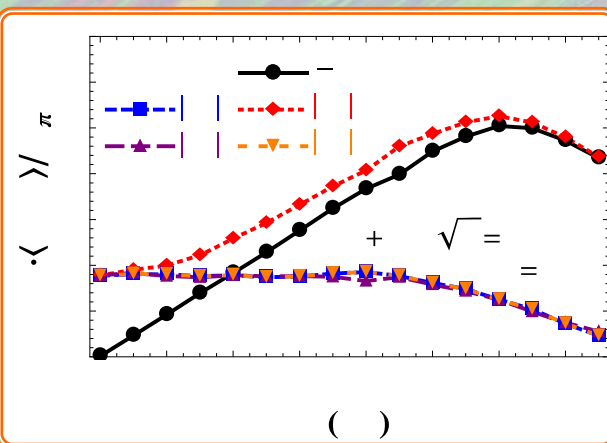


Event-by-event generation of electromagnetic fields in heavy-ion collisions

Direct calculations of Liénard-Wiechert potentials using coordinates and velocities of incoming protons* from HIJING

Wei-Tian Deng and Xu-Guang Huang, Phys.Rev. C85 (2012) 044907

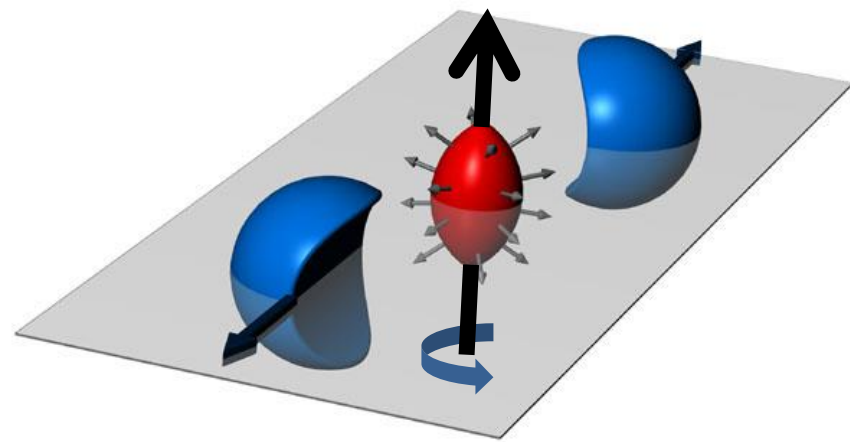
$$e\mathbf{E}(t, \mathbf{r}) = \frac{e^2}{4\pi} \sum_n Z_n \frac{\mathbf{R}_n - R_n \mathbf{v}_n}{(R_n - \mathbf{R}_n \cdot \mathbf{v}_n)^3} (1 - v_n^2),$$
$$e\mathbf{B}(t, \mathbf{r}) = \frac{e^2}{4\pi} \sum_n Z_n \frac{\mathbf{v}_n \times \mathbf{R}_n}{(R_n - \mathbf{R}_n \cdot \mathbf{v}_n)^3} (1 - v_n^2),$$



The electromagnetic fields at $t = 0$ and $r = 0$ as functions of the impact parameter b
Due to EbyE fluctuations $\langle |E_x| \rangle \approx \langle |E_y| \rangle \approx \langle |B_x| \rangle \neq 0$

*Contributions from the produced partons to the generation of the EM field is neglected.

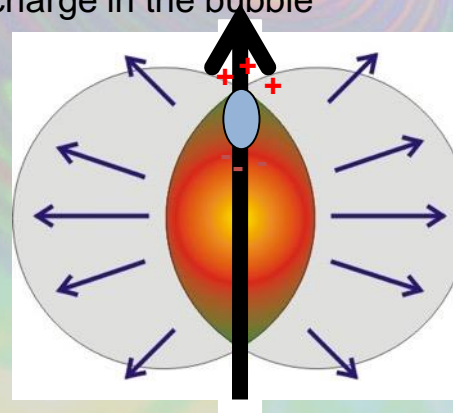
Separation of Charge wrt the reaction plane



- The signal is manifestly parity odd
 $x \Rightarrow -x, p \Rightarrow -p$
but the observable will be even
- The charge-flow asymmetry is too small to be seen in a single event but may be observable with correlation techniques

If a chirally restored bubble is created in a heavy ion collision, the positively charged quarks will go up ... then hadronize ... and yield an excess of positive pions above the plane

Unfortunately, it could be just the opposite in the next event depending on the topological charge in the bubble



Feed-down complication

- Most of our Lambdas are not emitted directly from the plasma.
- Significant feed-down from (polarized) parents complicates the picture
- Still a linear relationship (for small polarization)

Becattini, Karpenko, Lisa, Uspal, Voloshin PRC95 (2017) 054902

$$\begin{bmatrix} \frac{W}{T} \\ \frac{B}{T} \end{bmatrix} = \begin{bmatrix} \frac{2}{3} \sum_R \left(f_{LR} C_{LR} - \frac{1}{3} f_{S^0R} C_{S^0R} \right) S_R (S_R + 1) \\ \frac{2}{3} \sum_R \left(f_{L\bar{R}} C_{L\bar{R}} - \frac{1}{3} f_{\bar{S}^0\bar{R}} C_{\bar{S}^0\bar{R}} \right) S_{\bar{R}} (S_{\bar{R}} + 1) \end{bmatrix} m_R \quad \begin{bmatrix} \frac{-1}{P_L^{\text{meas}}} \\ \frac{1}{P_{\bar{L}}^{\text{meas}}} \end{bmatrix}$$

overall, ~15% effect

f_{LR} = fraction of Ls that originate from parent $R \rightarrow L$

C_{LR} = coefficient of spin transfer from parent R to daughter L

f_{S^0R} = fraction of Ls that originate from parent $R \rightarrow S^0 \rightarrow L$

C_{S^0R} = coefficient of spin transfer from parent R to daughter S^0